

We are IntechOpen, the world's leading publisher of Open Access books Built by scientists, for scientists

6,900

Open access books available

186,000

International authors and editors

200M

Downloads

Our authors are among the

154

Countries delivered to

TOP 1%

most cited scientists

12.2%

Contributors from top 500 universities



WEB OF SCIENCE™

Selection of our books indexed in the Book Citation Index
in Web of Science™ Core Collection (BKCI)

Interested in publishing with us?
Contact book.department@intechopen.com

Numbers displayed above are based on latest data collected.
For more information visit www.intechopen.com



Contribution of Satellite Measurements to the Modeling and Monitoring of the Quality of Coastal Seawater

Houma Fouzia, Bachouche Samir,
Bachari Nour El Islam and Belkessa Rabah

Additional information is available at the end of the chapter

<http://dx.doi.org/10.5772/53375>

1. Introduction

The highly demographic increase in the developing countries led to a rapid expansion of the primary urban areas. Solid and liquid rejects coming from domestic consumption and industrial activities are spilled out on potential water sources such as seas, lakes and other natural areas. In order to protect the natural medium and to control the pollution caused by such rejects. It is necessary to achieve a continuous survey of the reject zones. Satellite imagery can be used to estimate, with a reasonable accuracy, the factors affecting the water quality. It has a great importance to achieve the necessary continuous monitoring of the relevant area with an overall analysis of its pollution. (Houma F and al, 2004)

Waste disposal in water affects and alters the chemical and physical characteristics of the water in question, consequently its light reflectance properties which can be detected by satellite imagery. These changes cause, in turn, an alteration of the water appearance. It is, therefore, reasonable to estimate the relations linking the variation of the chemical and physical properties to the variation of the spectral properties of water, or more precisely, to its reflecting power.

Water was sampled from sites of Oran and Algeria's bay, port, sea, as well as from the urban sewage and industrial refuse. Temperature (T), acidity (pH), turbidity (TU), suspended material (SM), dissolved oxygen (DO), electrical conductivity C, chemical oxygen demand (COD), biological oxygen demand at the fifth day (BOD₅) and reflectance of water from satellite SPOT were determined.

The reflectance coefficient of water at each of the studied areas has calculated using SPOT image at three bands: XSI (0.5 - 0.59 μm), XS2 (0.6 - 0.69 μm) and XS3 (0.7 - 0.79 μm). The aim

of this study is to find the regression line (equation) and the correlation between the reflectance coefficient, calculated from satellite image, and each physical and chemical parameter.

The sea water pollution by hydrocarbons became alarming, considering the harmful effects caused on the environment. Pollution by hydrocarbons is the technological risk the most threatening in the area of Algiers due to the existence of a particularly polluting industrial zone at the origin of which a great sea traffic.

The satellite images however are the most used by the researchers to determine these pollutants, considering the width of the field of sight and the radiometric range of the satellites which extends from the visible to the infra-red and until the radar image.

In this work, we were interested to combine the information required by various satellites to characterize the sea water pollution by hydrocarbons. The optical images used are collected by the satellites Landsat *MSS*, *TM* and *SPOT*. The detection and the possible determination of the zones contaminated by hydrocarbons using the space techniques constitute an effective means to intervene in order to ensure the monitoring of the Algerian coasts.

A correlative analysis between the hydrocarbon contents and the reflectance calculated by the satellite images allow us to transform rough images into images treated and combined using a software of satellite image processing *PCSATWIN*. These images delimit and characterize the zones polluted by hydrocarbons.

Indeed, our objective consists of the development of a methodology based on the satellite data for the localization and the monitoring of the evolution of pollution by *polyaromatic and total hydrocarbons*. The analysis shows us that each sensor offers useful information and that the combination between these various informations makes it possible to propose a procedure of maps establishment that can be interpreted as aquatic pollution maps. (Spitzer & Dirks, 1985 ; Baban ,1993 and Houma et al., 2010).

2. Analysis on the ground and water sampling

Knowledge of the water quality is an essential component in integrated coastal management. Direct supervision increased, coupled with the reflectance of the sea calculated from satellite sensors is necessary to determine the status of coastal waters.

We present the methodology used for modeling of chlorophyll and the phytoplankton that have an effect on the color and quality of marine waters. The use of satellite imagery has allowed mapping of parameters indicative of water pollution and photosynthetic organisms on the surface and at depth. The objective of the work is twofold:

- Get models between the spectral response of seawater with the physical properties of optical pollution parameters using ground measurements.
- Perform inversion models in order to achieve a mapping of the spatial and temporal variability of parameters in surface water and into the depths of coastal areas.

The coastal zone water is the most significant part of the sea from nutritive resources point of view but also most subjected to the aggressions of pollution of various natures. The Algiers littoral is practically touched by various types of pollution. We note a significant urban density on the coast which pours its discharges in marine water and of the factories which reject their industrial waste and contribute to pollute the environment under the effect of the toxic and corrosive substances in addition to the very significant sea traffic present in the area.

The use of the remote sensing can advantageously replace the long, expensive and tiresome traditional methods for the monitoring of the quality of water.

The taking of images has encouraged the scientists to its use in various applications in marine sciences. The techniques used rest on a simple and effective concept which is to correlate the satellite data with in situ measurements. (Houma F and al, 2010)

The Algiers bay is located in the central part of the Algerian coast. It is characterized by its semicircular shape of an approximate surface of about 180 km². It is limited to the East by Bordj El- Bahri (Cape Matifou) and to the West by Rais Hamidou (the Pescade headland). This area is very urbanized and the majority of the units are concentrated in the industrial zones of Oued Smar, El Harrach, Algiers seaport, Rouiba and Réghaia. The city is located on the Mediterranean coast, in the North of Africa with a latitude of 36° 49' 35'' - 36° 49' 50'' and longitude of 03° 14' 50'' - 03° 00' 40'' East. The zone of study is mainly contaminated by various sources of pollution and is subjected to several types of urban, industrial and oil wastes.

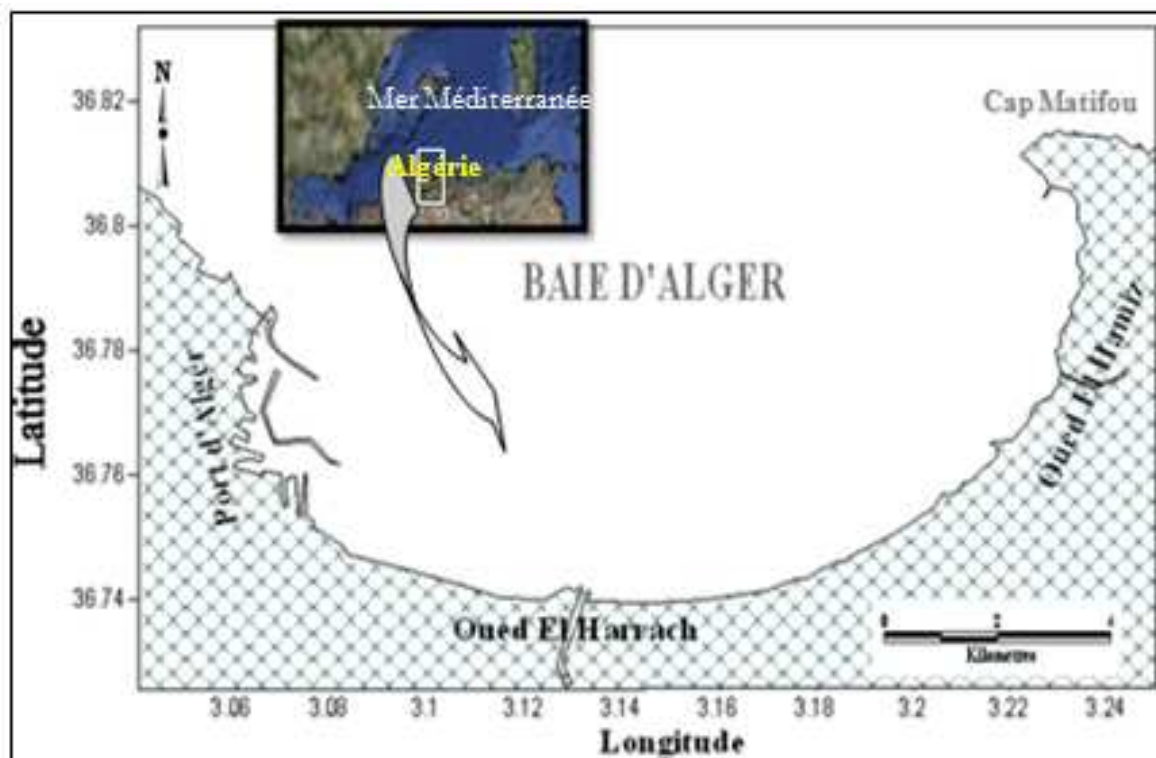


Figure 1. Location of the Bay of Algiers

Within the evaluation framework of the coastal site contamination degree of Algiers bay by hydrocarbons. The analyses are carried out at the laboratory by applying the method "ultra-violet Spectrofluorimetry" for the polyaromatic ones and "the infra-red" for total hydrocarbons.

The choice of the site is not fortuitous; indeed studies on Algiers bay show clearly that all the coast is polluted by hydrocarbons.

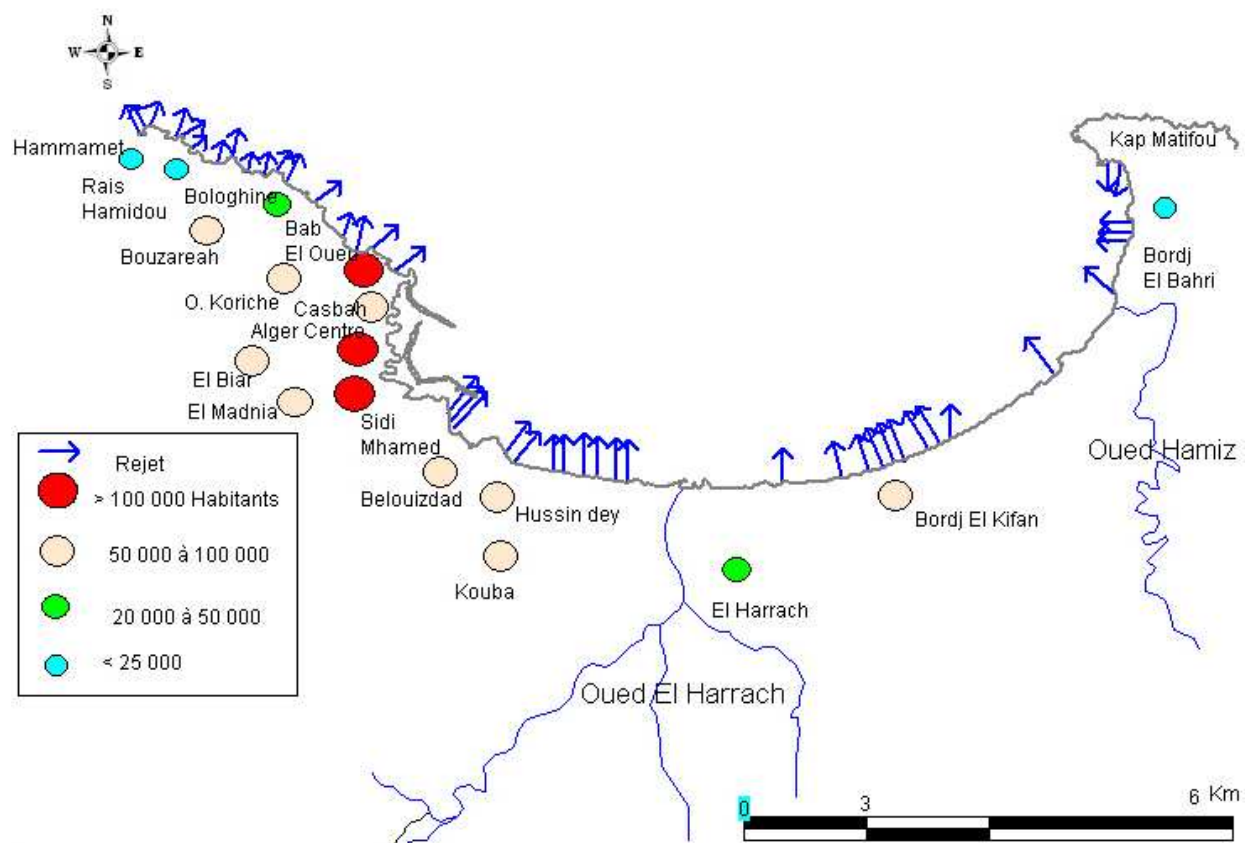


Figure 2. The main sewage discharges in the Bay of Algiers.

Since the first inhabited flights, studies on the quality of littoral water were identified according to their turbidity, in particular on the basis of the images acquired by *the Gemini* capsules correlated with in situ measurements. Since 1970, several scientists observed a positive correlation between the signal received by the sensor and the suspended matter content. The turbidity cartography of the surface and the estimate of the matters suspended based upon reflectance were carried out by Spitzer et Baban. These works rest on the strong correlation observed between the images and the content of these measured concentrations *in situ*. A significant correlation between the numerical account of the first channel of the satellite Landsat TM and the suspended matter concentration was carried out.

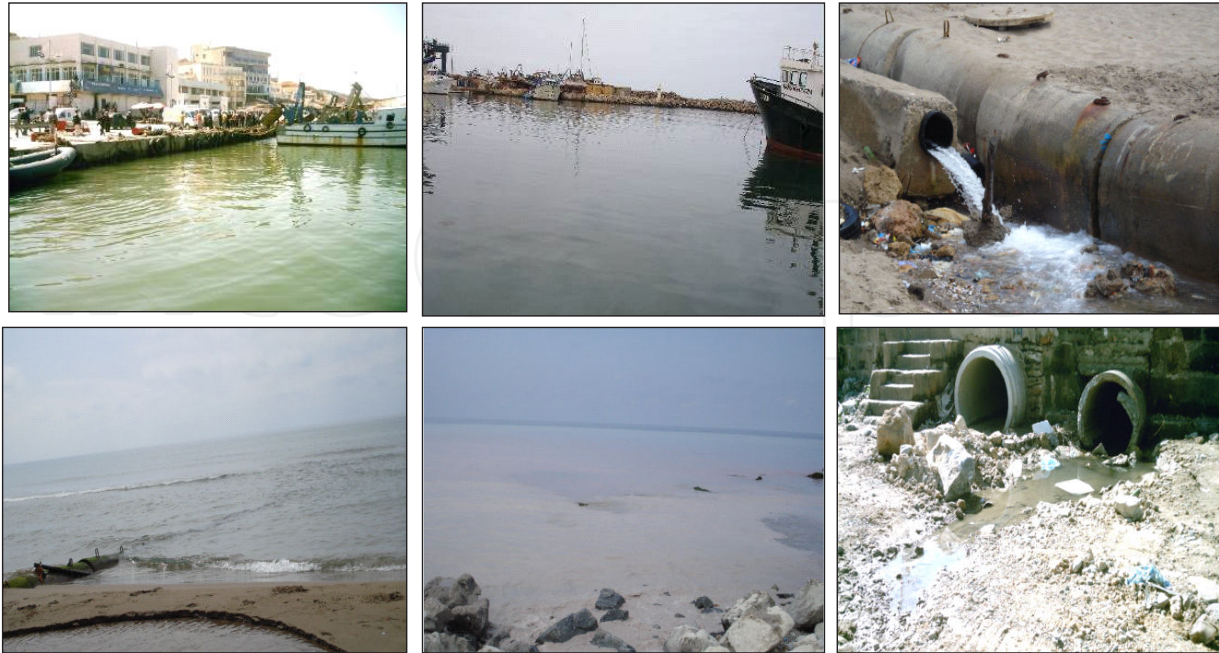


Figure 3. Oil pollution, industrial and urban discharges the level of the Bay of Algiers

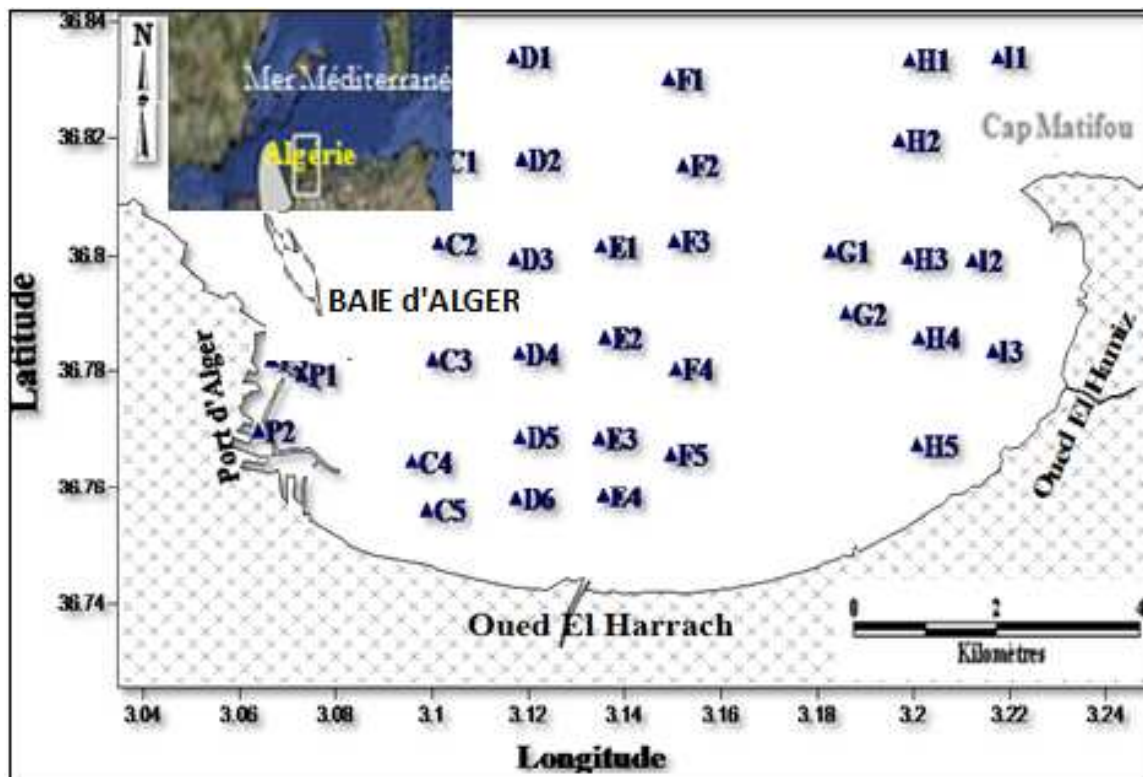


Figure 4. Location of sampling stations during of the oceanographic cruise 2009

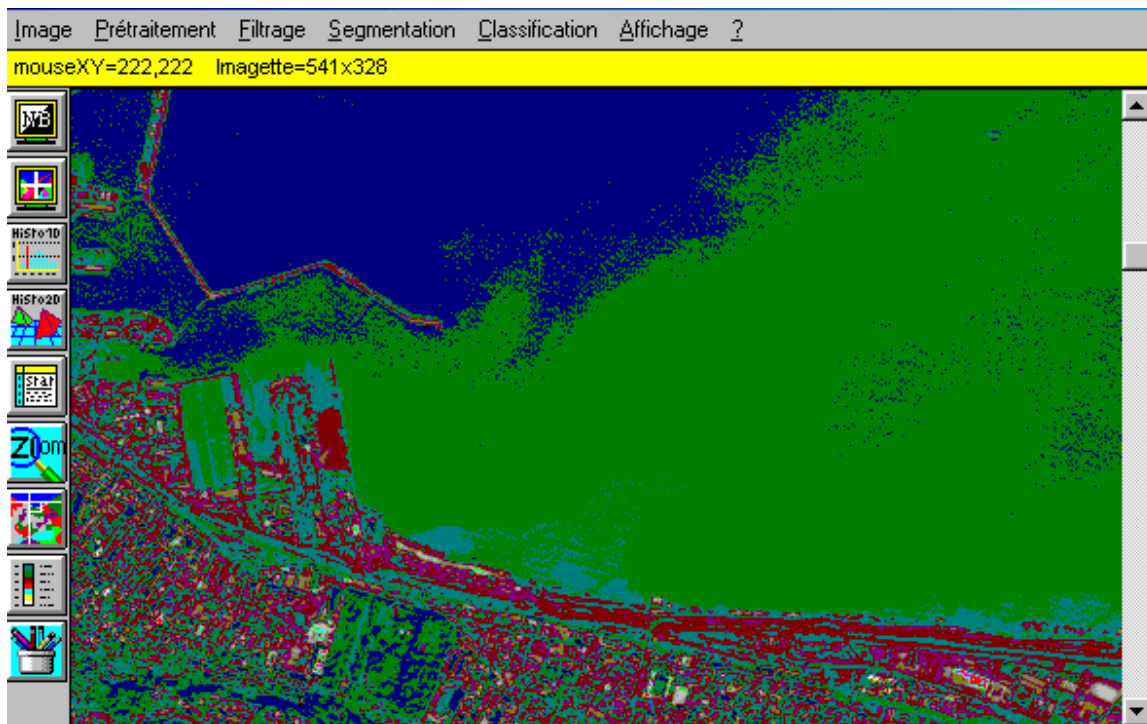


Figure 5. Rough image of bay of Algiers taken by the satellite SPOT.

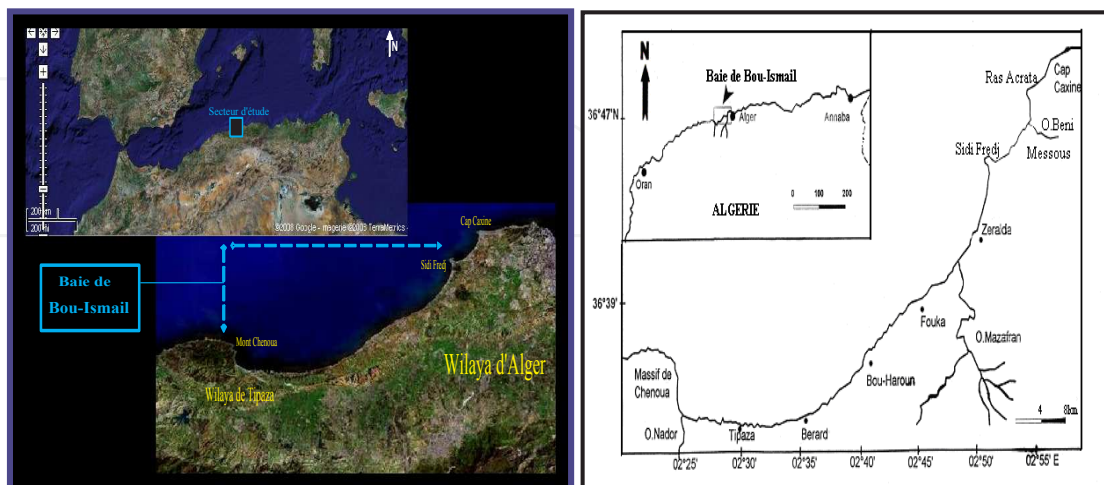


Figure 6. Geographical location of the Bay of Bousmail



Figure 7. The main sewage discharges in the Bay of Bousmail

The spectral bands *Thematic Mapper* were used more to correlate with the spectral properties of water and its content in organic matter or for the characterization of the colour, salinity and the sea water chlorophyll concentration.

While taking as a starting point the various developed approaches and the characteristics of the satellites SPOT and Landsat, we have tried to highlight the use of the teledetection in order to find relations between the optical parameters and the hydrocarbon concentration present in water.

A model of interaction of the solar spectrum with the system ground-atmosphere-sensor is thus developed in order to transform the rough images into reflectance images.

The results of reflectance obtained from the numerical data SPOT and Landsat are correlated with the results expressing the content of polyaromatic and total hydrocarbons. The relations of the correlative analysis are given in each spectral band of the satellites to distinguish the best coefficients of correlation and then to apply the best adjustment in order to transform a rough image into indicating image of pollution.

3. Determination of water reflectance by SPOT imagery

Radiation reaching the satellite is made up of the global spectral radiation reflected by the ground while passing again through the atmosphere $R_{\text{ground-atm}}$ and part of diffused radiation by the Earth's atmosphere towards the satellite $R_{\text{atm-sat}}$; the radiation which reaches the sensor is:

$$\begin{aligned}
 R_{\text{sensor}} &= R_{\text{ground-atm}} + R_{\text{atm-sat}} & \text{a} \\
 R_{\text{sensor}}(\lambda) &= R_{\text{atm-sat}}(\lambda) + G_{\lambda}(\theta_s) T_{\lambda}(\theta_v) \rho_l & \text{b}
 \end{aligned}
 \tag{1}$$

With:

$$\begin{aligned}
 R_{\text{ground-atm}} &= G_{\lambda}(\theta_s) T_{\lambda}(\theta_v) \rho_{\lambda} / (1 - \rho_{\lambda} \omega) & \text{a} \\
 R_{\text{sat}} &= E_{\text{atmo}} + G(\theta_s) T_{\lambda}(\theta_v) \rho_{\lambda} & \text{b}
 \end{aligned}
 \tag{2}$$

ρ_{λ} is the coefficient of reflectance, G_{λ} is the total radiation which reaches the ground, it represents the sum of a direct radiation and a radiation diffused by the air molecules and the aerosols towards the ground; $T_{\lambda}(\theta_v)$ is the function of the radiation transmission into upper atmosphere; ω is the spherical albedo for the atmosphere which explains the multiple reflexions between the surface of the ground and the atmosphere; θ_s is the solar angle of zenith in degrees and θ_v is the angle of sight of the sensor at the time of while taking the images. (Houma and Bachari, 2012)

Since the reflectivity of water is low, the equation (1) can be roughly linear as in equation (1b):

The radiance of measured by a satellite sensor results from the solar radiation affected by several process: absorption and diffusion on both downward and upward path by the atmospheric components, reflection at the ground surface.

where: E_{atmo} is just the radiance of the atmosphere if the ground was nonreflecting ($\rho_{\lambda} = 0$); G_{λ} is a global radiation include a direct radiation and a diffuse radiation.; $T_{\lambda}(\theta_v)$ is a transmission function from the ground to the top of the atmosphere for the radiance; ρ_{λ} is the hemispherical reflectance of the ground, A is the spherical albedo for the atmosphere which account for multiple scattering and reflections between the ground surface and the atmosphere; θ_s solar zenith angle in degrees and θ_v viewer angle in degree

When the soil reflectance is a weak the equation (1) can be approximately in linear form as in equation (2b):

The SPOT satellite observes the earth, in three spectral channels XS1 (0.5 - 0.59 μm), XS2 (0.6 - 0.69 μm), XS3 (0.7 - 0.79 μm) with a spatial resolution of 20m and with a panchromatic channel (0.6 - 0.81 μm) with a spatial resolution 10m. In these SPOT spectral windows, only ozone absorption, molecular and aerosol diffusion, affect radiation in its double way sun-ground and ground-captor (Bachari.N et al, 1997).

In the first part of our work we simulate the measurement achieved by the captor for pure water (from the sea far from any pollution).

$$\begin{aligned}
 B_{\text{simulated}} &= \frac{\int_{\Delta\lambda} R_{\text{sat}\lambda} S_{\lambda} d\lambda}{\int_{\Delta\lambda} E_{0\lambda} (1 + f) \cos(\theta) S_{\lambda} d\lambda} & \text{a} \\
 B_{\text{simulated}} &= C_J \cdot B_{\text{image}} & \text{b}
 \end{aligned}
 \tag{3}$$

where $E_{0\lambda}$ is a mean solar exo-atmospheric irradiances in $w\text{ cm}^{-2}\ \mu\text{m}^{-1}$; $(1+f)$ is an earth-sun distance in astronomical units. The “ f ” for a specific day can be approximated by the relation of Gurney and Hall,1983; $f = 0.0167 \sin(2\pi (j - 93.5))/365)$ where j is day number of the year, S_λ : is a sensitivity of record and $\Delta\lambda$ is a band of record.

In second part we using the imagery treatment (N.Bachari et al, 1994), we determine the real value evaluated by the satellite for a deep sea water (B_{real}). We use a both the simulated value ($B_{\text{simulated}}$) and the real value to calculated the calibration C_j factor for each channel :

$$C_i = (B_{\text{simulated}} / B_{\text{real}})_i \quad (4)$$

We take the image and we transform the digital account into radiance by the linear relation :

$$E = \pi \cdot C_j \cdot B \quad (5)$$

for each channel j We use the reverse model to calculate the reflectance Ref_j for each pixel from the following relation:

$$\begin{aligned} Ref_j &= \frac{\pi C_j B - \int_{\Delta\lambda} R_{atmo} S_\lambda d\lambda}{\int G_\lambda T_\lambda(\theta_v) S_\lambda d\lambda} & a \\ E = \pi L &= A + K \langle \rho \rangle & b \\ \Pi L &= R_{atm-sat} + R_{sol-atm} & c \\ \Pi L &= A + K \langle \rho \rangle & d \end{aligned} \quad (6)$$

The brightness simulated in the general case is given by:

$$B_{\text{simulated}} = \frac{\int R_{\text{sensor}(\lambda)} \cdot S(\lambda) \cdot d\lambda}{\int_{\Delta\lambda} S(\lambda) d\lambda} \quad (7)$$

$S(\lambda)$ represents the spectral band.

If the real brightness of a given image is B_{image} , we must have a first order relation of approximation such as in equation (3b)

$$\begin{aligned} A &= \frac{\int_{\lambda_1}^{\lambda_2} R_{\text{capteur}} S(\lambda) d\lambda}{\int_{\lambda_1}^{\lambda_2} S(\lambda) d\lambda} \quad , \text{and} : \quad K = \frac{\int_{\lambda_1}^{\lambda_2} G_\lambda T_\lambda S(\lambda) d\lambda}{\int_{\lambda_1}^{\lambda_2} S(\lambda) d\lambda} \\ B_{\text{image}} &= \frac{\int_{\Delta\lambda} R_{\text{sensor}(\lambda)} \cdot S(\lambda) d\lambda}{\int_{\Delta\lambda} E_0(\lambda)(1+f)\cos(\theta)S(\lambda)d\lambda} \end{aligned} \quad (8)$$

C_j is the factor of calibration of the sensor; $E_0(\lambda)$ is the average radiance outside the solar atmosphere expressed in unit $W\ cm^{-2}\ \mu m^{-1}$; $(1+f)$ is the distance earth-sun in astronomic units; f is the coefficient given by the relation of "Gurney and Hall, (1983)" such as for one day specific: $F = 0.0167 \sin(2\pi (J - 93.5)/365)$ where J is the number of days of the year.

3.1. Rough satellite data conversion into reflectance

The calibration of the numerical accounts in reflectance of the set ground and atmosphere is carried out according to the method suggested by the users guide Spot. It is obtained by a linear transformation of numerical accounts into brightness:

$$L = CN/G \quad (9)$$

Where: L : is brightness in $W/m^2/Sr$; N : the numerical account

G : the gain of the sensor absolute calibration

For an application in images, it is thus necessary to be able to transform values of brightness into numerical account then in reflectance values and that by taking into account a considerable zone representing the sea in a given scene. Knowing the values of brightness for a given channel and each type of sensor, the data is expressed in milliwatts per centimetre square per steradian by micrometer ($W/m^2/Sr$).

The passage to reflectance values is done in two stages:

- Brightness conversion L_λ into numerical account CN .
- Conversion into reflectance Ref on the level of each pixel.

The relation between the numerical account of a pixel CN and its brightness on the level of the sensor is linear. We can write the relation in the form:

$$L_\lambda = a \cdot CN + a_0 \quad (10)$$

a and a_0 are called coefficients of calibration.

By making an approximation to this function which represents a whole of numerical data by an analytical function we could have the following relation:

$$CN_{XS1} = 1,23 \cdot L_{XS1} - 0,22$$

For the same conditions of simulation, the constants are calculated by using the spectral signatures of sea water for the data of the channels. For HRV SPOT, the results are reproduced in the following table:

Channel	a	a ₀
XS1	1,23	0,22
XS2	1,24	-0,08
XS3	1,32	-0,59

Table 1. Coefficients of calibration for HRV SPOT.

Combining between the equations which express spectral brightness and reflectance on the level of the ground, we find also a linear relation between the numerical account and the reflectance Ref which can be written in the form:

$$\text{Ref} = b \cdot \text{CN} + b_0 \quad (11)$$

In this case term Ref contains all the informations on the optical properties and the terrestrial scene observed. The parameters b and b₀ depend on the atmospheric and astronomical conditions.

We present the graph determining the linear relation of calibration between the reflectance and the numerical account for the channels of SPOT XS1, XS2 and XS3.

Application:

	L(w.m ⁻²)	CN	Ref.
Channel XS1	53.935	66.560	0.3215
Channel XS2	17.734	21.910	0.2606
Channel XS3	6.0591	7.408	0.2101

Paramètres atmosphériques		Paramètres astronomiques	
Ozone Cm	0.30	Jour	344
Humidité relative %	80	Heure	11.26.00
Température K	T°C+273	Latitude	36°38'58.67"N
Visibilité Km	20	Longitude	2°24'2.45"E
Altitude de l'ozone	200	β ₀	0
Alpha (α)	1.5	θ _v	10°
F _c	0.9	φ	45°
ω ₀	0.9	ψ	60°

- The reflectance of water is strong in the first channel compared to the second channel where it is also more significant as that calculated in the channel three.
- The reflectance of the zones loaded with sediments and that of the polluted zones is stronger compared to the reflectance of the water zones not loaded.

Table 2. The input parameters for the SDDS

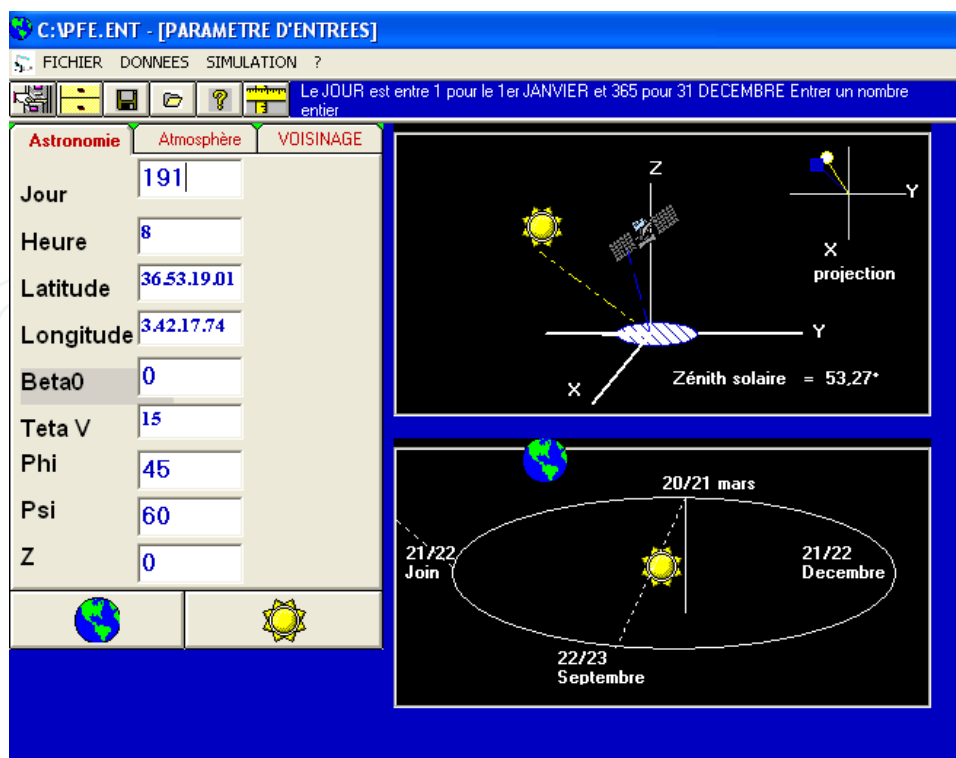


Figure 8. Atmospheric and astronomical data by SDDS software

Téta V		10			20		
Stations	Prof	SPOT 1	SPOT 2	SPOT3	SPOT 1	SPOT 2	SPOT 3
1	1	49,463	23,237	5,2607	49,401	23,536	5,3053
2	1,5	48,476	21,265	5,0766	48,435	21,544	5,0993
3	1,5	48,451	21,692	5,2331	48,412	21,975	5,2583
4	1,5	48,451	21,692	5,2331	48,412	21,975	5,2583
5	1,5	48,996	21,938	5,2943	48,957	22,224	5,3198
6	2	47,567	19,736	4,9991	47,545	19,990	5,0104
7	2	47,567	19,737	5,0061	47,545	19,991	5,0174
8	2	35,627	15,095	3,8516	35,612	15,289	3,8612
9	4	44,602	16,728	5,0852	44,668	16,884	5,0860
10	4,5	43,973	16,279	5,0888	44,020	16,414	5,0892
11	4,5	43,965	16,271	5,0829	44,012	16,406	5,0832
12	4,5	43,985	16,291	5,0971	44,032	16,427	5,0974
13	5	32,129	10,226	2,3493	32,093	10,306	2,3495
14	5	32,303	10,156	2,3292	32,266	10,235	2,3293
15	5	32,129	10,226	2,3493	32,093	10,306	2,3495
16	5	32,481	11,916	3,8032	32,524	12,002	3,8034
17	5,5	31,71	10,014	2,3491	31,684	10,083	2,3492
18	6	31,313	9,8473	2,3490	31,295	9,9059	2,3491
19	8	29,908	9,4613	2,3490	29,917	9,4914	2,3490
20	8,5	29,912	11,107	3,8071	29,992	11,134	3,8071

Table 3. Luminances L (w.m⁻²) on the three channels SPOT HRV

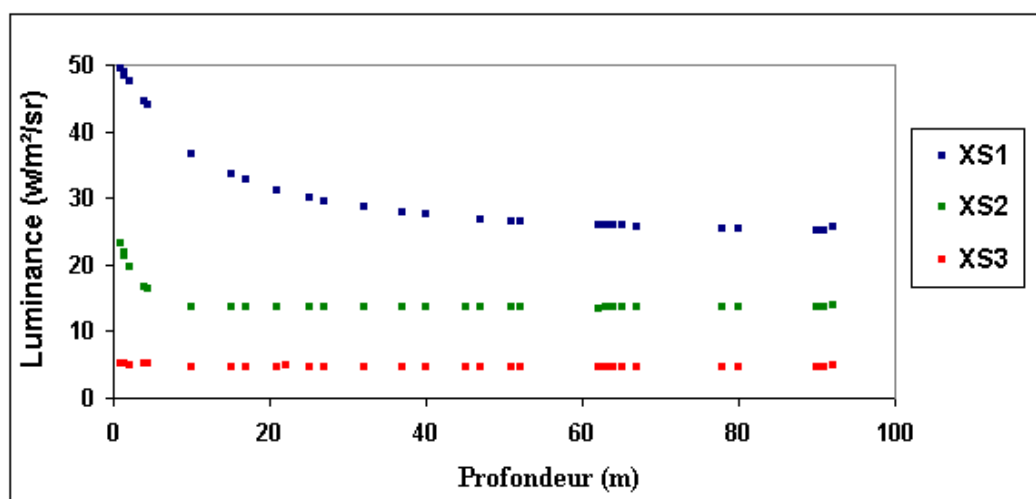


Figure 9. The reflectance in the the water column on the channels (SPOTXS). (Houma et al,2010)

4. Determination of water reflectance by SPOT imagery

The radiance of measured by a satellite sensor results from the solar radiation affected by several process: absorption and diffusion on both downward and upward path by the atmospheric components, reflection at the ground surface. The SPOT satellite observes the earth, in three spectral channels XS1 (0.5-0.59 μm), XS2 (0.6-0.69 μm), XS3 (0.7-0.79 μm) with a spatial resolution of 20m and with a panchromatic channel (0.6 - 0.81 μm) with a spatial resolution 10m. In these SPOT spectral windows, only ozone absorption, molecular and aerosol diffusion, that affects radiation in its double way sun-ground and ground-captor (Bachari.N et al, 1996).

The SPOT satellite observes the earth, in three spectral channels with a spatial resolution of 20m and with a panchromatic channel (0.6 - 0.81 μm) with a spatial resolution 10m. In these SPOT spectral windows, only ozone absorption, molecular and aerosol diffusion, affect radiation in its double way sun-ground and ground-captor (Bachari.N et al, 1996).

In the first part of, we simulate the measurement achieved by the captor for a pure water (from the sea far from any pollution).

Turbidity and suspended solids have one comment effect in reducing light penetration thereby suppressing primary production in the form of algae and macrophates. This, in turn affects the available dissolved oxygen.

The oxygen needed for chemical oxidation of organic matter and the accompanied minerals is expressed as COD. Therefore, higher values of this parameter means more organic pollution. BOD₅ estimates the oxygen needed for biological oxidation of organic and inorganic matters by organisms which are actually present in the polluted water. So, the ratio COD/ BOD₅ refers to the capacity of organisms found in the water to oxidise the organic matter found in the medium. For easier monitoring water quality we could use the satellite imagery to expect, by

excellent validity, the capability of the water to reduce the organic pollution resulted from urban discharge. Saprobity is a biocenotial expression of BOD_5 . Many investigators (Zelinka and Marvan, 1957; Rothshein, 1977 and Sladeczek, 1973) showed the relation of saprobic zones to the BOD_5 especially within the limosaprobity Sladeczek and Tucek (1975) modified this relation and showed the abundant organisms at different saprobic index. They reported that their diagram is valid in 90 - 95% of cases. According to Sladeczek (1969 and 1973), our BOD_5 values (50 - 500) represent saprobic index between 3.5 to 6.5 which have saprobity degrees of polysaprobity (sea in this work), isosaprobity (port, zone3 and P.lac1), and metasaprobity (outlet1, outlet2 and Plac2). According to Graham category (1965) our areas are seriously (sea, port, zone 3, and P.lac1) and grossly (outlet 1,outlet2 and P.lac2) polluted.

At such saprobic index the self purification and decay is going under anaerobic condition.

The substances which determine the optical properties of water surfaces, and then influence their reflectivity, may be classified in three categories : i) the alive phytoplankton and the detritus which come with it ;ii) the suspended particles; iii) the dissolved organic matter. The phytoplankton and the biogenic detritus which are associated with it have generally the same colour. In most oceanic waters and in some coastal waters where terrigenous supplies are little, the influence of the phytoplankton is dominant. In natural conditions; it is very difficult to dissociate the effects of the phytoplankton and those of the biogenic detritus on the coefficient of absorption for which only global estimations are made. The phytoplankton cells and the particles correspond to the biogenic detritus causing a Mie diffusion of the light which does not much depended on the wavelength. Therefore, the colour of water gradually takes a green shade with the increase of the phytoplankton concentration. As it was expected, our results show that for polluted waters.

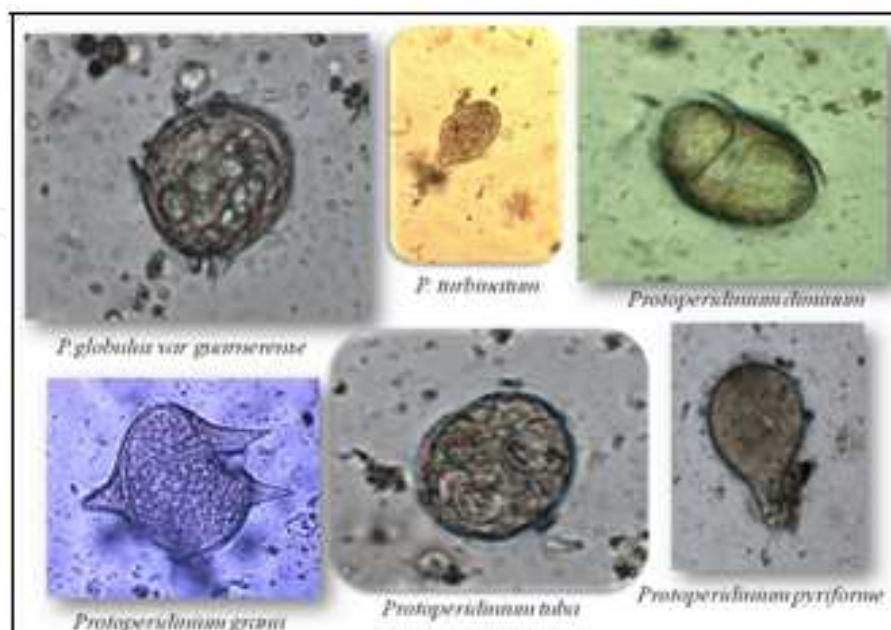


Figure 10. Phytoplankton species of genera (*Protoperidinium* et *Ceratium*) identified using an inverted microscope (Gx40).

A high correlation ($r = 0.65$) between turbidity and suspended material was found. Turbidity and suspended solids have one common effect in reducing light penetration thereby suppressing primary production in the form of algae and macrophytes. (Ferrari, 1992). This, in turn affects the available dissolved oxygen. Our results confirmed this situation which showed a high negative correlation between turbidity and dissolved oxygen ($r = 0.87$). The following regression equation is derived.

$$DO = -0.0252 Tu + 2.54552 \quad (12)$$

The oxygen needed for chemical oxidation of organic matter and the accompanied minerals is expressed as COD. Therefore a higher value of this parameter means more organic pollution. BOD₅ estimates the oxygen needed for biological oxidation of organic and inorganic matters by organisms which are actually present in the polluted water. So, the ratio COD/BOD₅ refers to the capacity of organisms found in the water to oxidize the organic matter found in the medium. The results showed that this ratio increased with pollution degree and with reflectance ($r = 0.9$) at the different reflectance channels. For easier monitoring water quality we could use the satellite imagery to expect, by excellent validity, the capability of the water to reduce the organic pollution resulted from urban discharge. Moreover, the biological parameters could be calculated from each other since they are highly correlated ($r^2 = 0.68 - 0.96$).

Saprobity is a biocenotic expression of BOD₅. Many investigators (Zelinka and Marvan, 1957; Rothschein, 1977 and Sladeczek, 1973) showed the relation of saprobic zones to the BOD₅ especially within the limosaprobity. Sladeczek (1975) modified this relation and showed the abundant organisms at different saprobic index. They reported that their diagram is valid in 90 - 95% of cases.

However, our results showed that the concentration of the dissolved oxygen in sea and port is moderate which means that the regression succession of saprobic cycle is continued under aerobic condition which may shorten this process toward less saprobity. It seems that the main sewage sites have reached the progressive direction of saprobity. It is now in the regressive succession of the saprobity and this process is more progressed in sea and port where more dissolved oxygen than in other areas where less dissolved oxygen. Outlet1,2 and Plac2 are suffering of the bad effect of both low dissolved oxygen and high turbidity.

The sites should be examined to determine the saprobity degree by biological indicators in order to know how the ecological system is developed.

According to a program developed by Bachari and Beabadji (1994), we used the equation

$$Ref2 = 0.0192 COD/BOD_5 - 0.0202 \quad (r^2=0.92) \quad (13)$$

to compose the figures 3 and 4 which clearly showed different distinct colour subareas in each of the studied area. Each colour indicates a different degree of water quality or pollution. By this technique it is possible to construct a very beautiful and global picture for degree of

unknown pollution spread over a wide water surface with relatively less expanses and rapid evaluation.

Correlation coefficient were very low ($r < 0.15$) between reflectance and some water physical parameters (T, pH and C).

However, reflectance was highly correlated ($r = 0.83 - 0.85$) with the rest of physical (TU, SM) and biological (DO, COD, BOD₅) parameters ($r = 0.67 - 0.92$).

Fonctions	Conversions radiométriques	R
Turbidité (NTU) = f (Ref TM1)	Turbidité (NTU) = $215,5\text{Ref}^2 + 231,6 \text{Ref} + 5,183$	+0,90211
Turbidité (NTU) = f (Ref XS1)	Turbidité = $315,9 \text{Ref (XS1)} - 1,670$	+0,88567
MES (mg/l) = f (Ref XS1)	MES (mg/l) = $439,1 \text{Ref(XS1)} - 3,611$	- 0,87023
Turbidité (NTU) = f (Ref TM2)	Turbidité = $131,1 \text{Ref (TM2)} - 1,059$	+0,84108
Ref (XS1) = f (Chlr)	Ref(XS1) = $0,17.\text{Ln(Chlr)} + 0,692$	+0,89532
Ref (TM1) = f (Chlr)	Ref(TM1) = $-1,224 * \text{Chlr}^2 + 1,224 * \text{Chlr} + 0,134$	+0,81403
Ref (TM2) = f (Chlr)	Ref(TM2) = $0,523 * \text{Chlr} + 0,168$	+0,76400

• Concentrations of chlorophyll a and suspended matter are specified in units mg/l.

Table 4. Correlations of reflectances and indicators for pollution of seawater obtained from the visible channels (SPOTXS) in the Algiers Bay. Database (Oceanographic Campaigns 2009)

5. Pollution map

By using software PCSATWIN we have transformed the reflectance image into an image which makes it possible to estimate a certain extent the pollution of the environments. Indeed, there is a strong relation between the reflectances and these components content. Actually, the colour of sea water which is one of the obvious organoleptic descriptors, remains always a significant factor of differentiation which informs about the gleam of water, about its quality and which can be useful like an indicator of its transparency.

However, it seems that the correlation is better for XS1 than XS2, and XS2 than XS3 on the satellite SPOT HRV. Landsat TM gives a strong connection on the first two channels while sensor MSS4 presents only the channel interesting for our application.

Spectral bands XS1, TM1, TM2 and MSS4 give the best coefficients of correlation with corresponding reflectances Ref (XS1), Ref (TM1), Ref (TM2) and Ref (MSS4). They are thus best adapted for the follow-up of the quality of water. The lowest values are observed on channels XS3, TM5, TM6, MSS6 and MSS7 what is entirely logical since the absorption of water becomes very significant in this infra-red band, on the other hand the diffusion of the radiation becomes very weak and almost negligible what decreases the information acquired by the sensors.

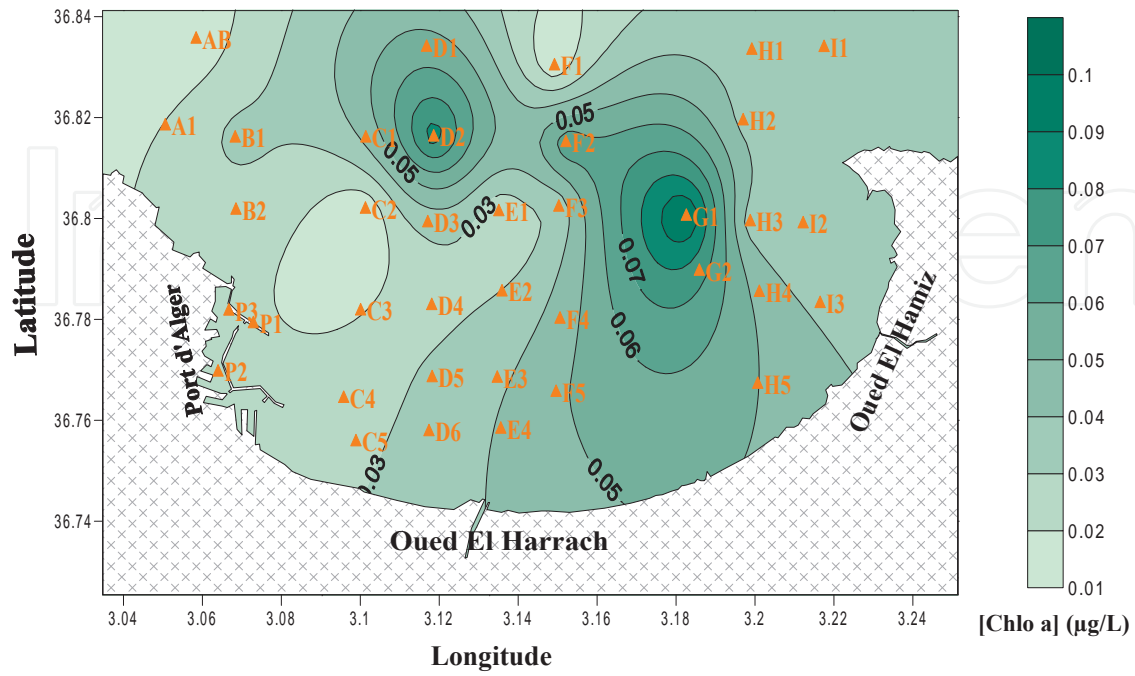


Figure 11. Spatial distribution of chlorophyll at 25 meters of depth in the bay of Algiers. (April, 2009)

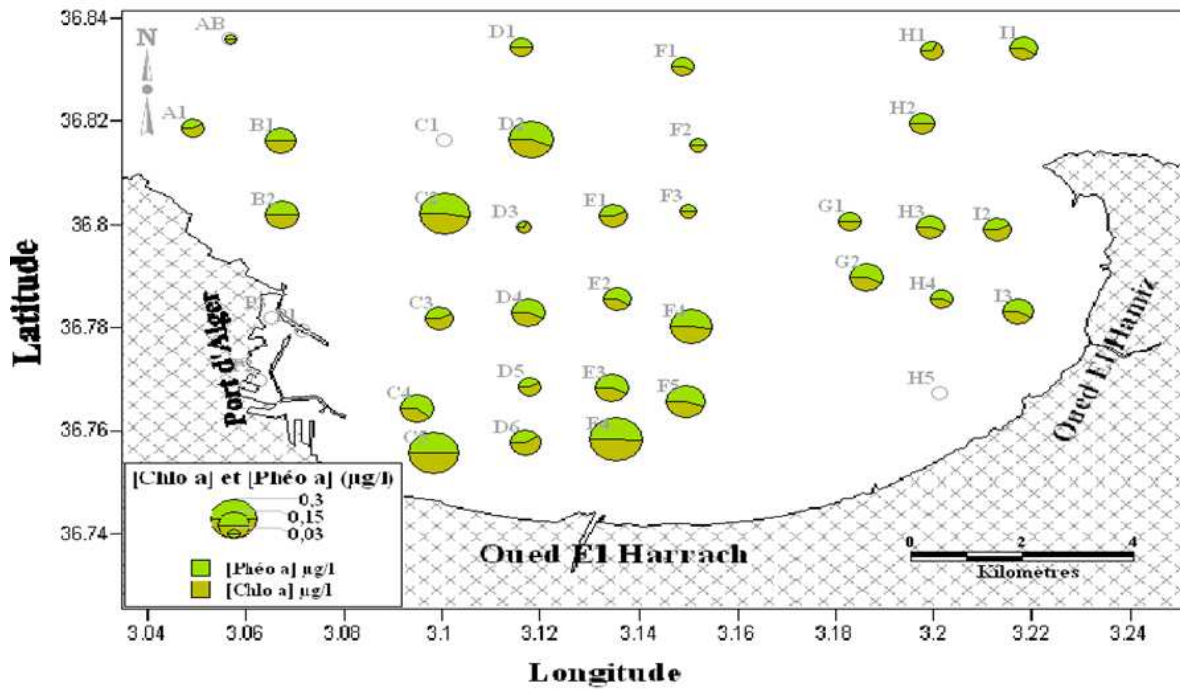


Figure 12. Distribution of chlorophyll a and pheopigments in surface waters of the Algiers Bay. (Oceanographic campaign in May 2009)

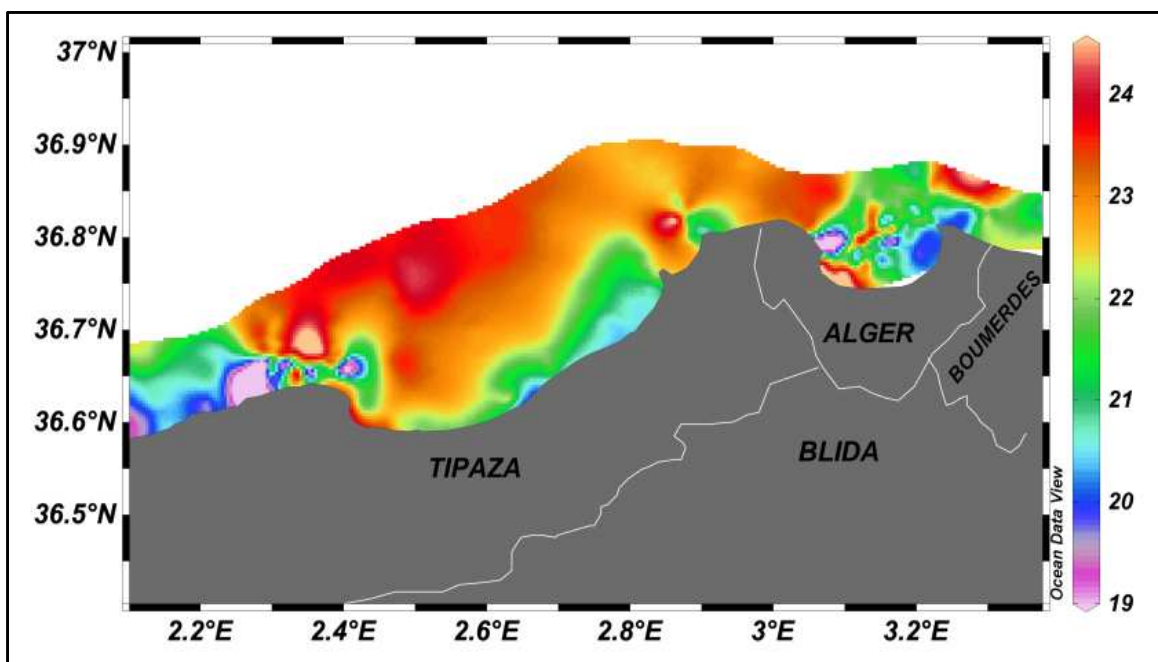


Figure 13. Variation of the temperature of the surface in the region Algiers.

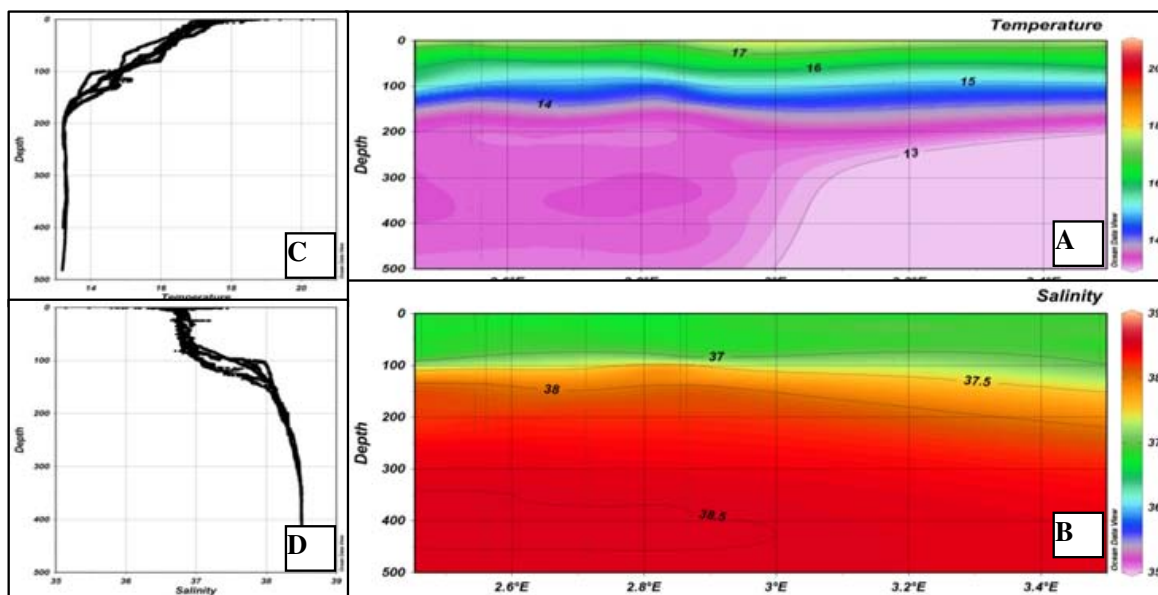


Figure 14. Temperature and salinity along the coast of the central region, profile of the temperature and salinity according to the depth.

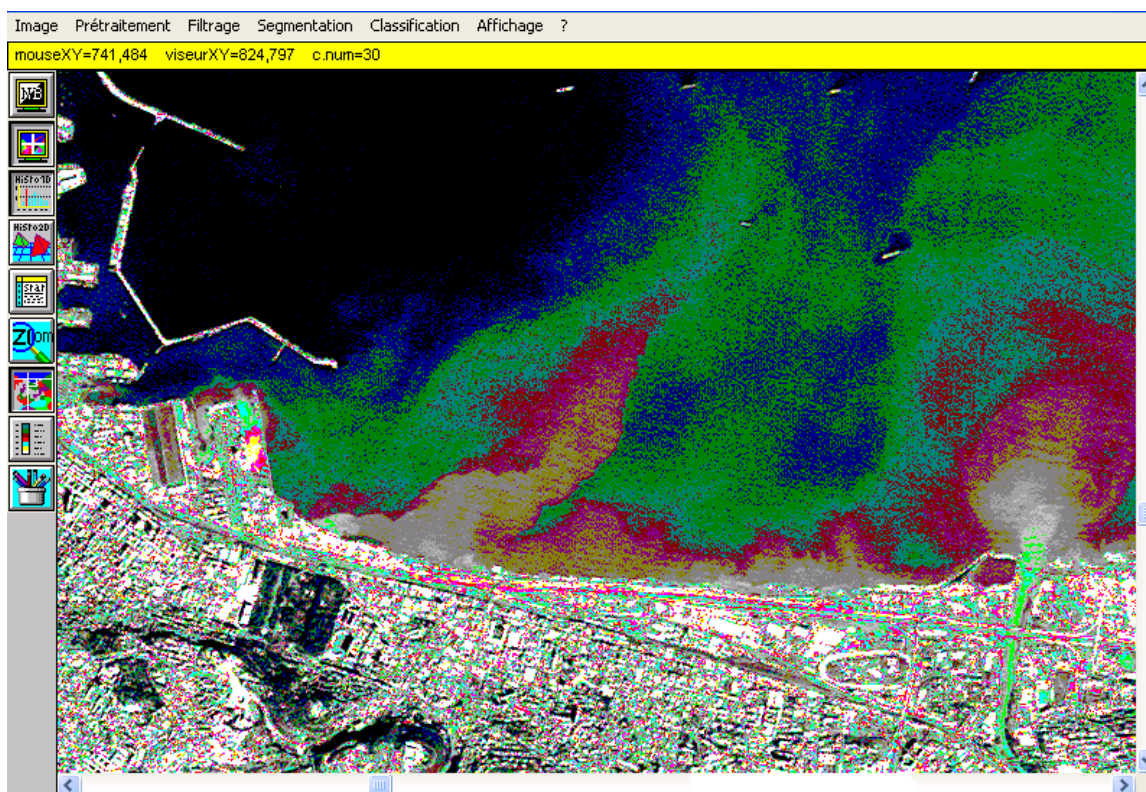


Figure 15. Variation of suspended matter on a SPOTXS satellite image of the Algiers Bay. (10 April 2009)

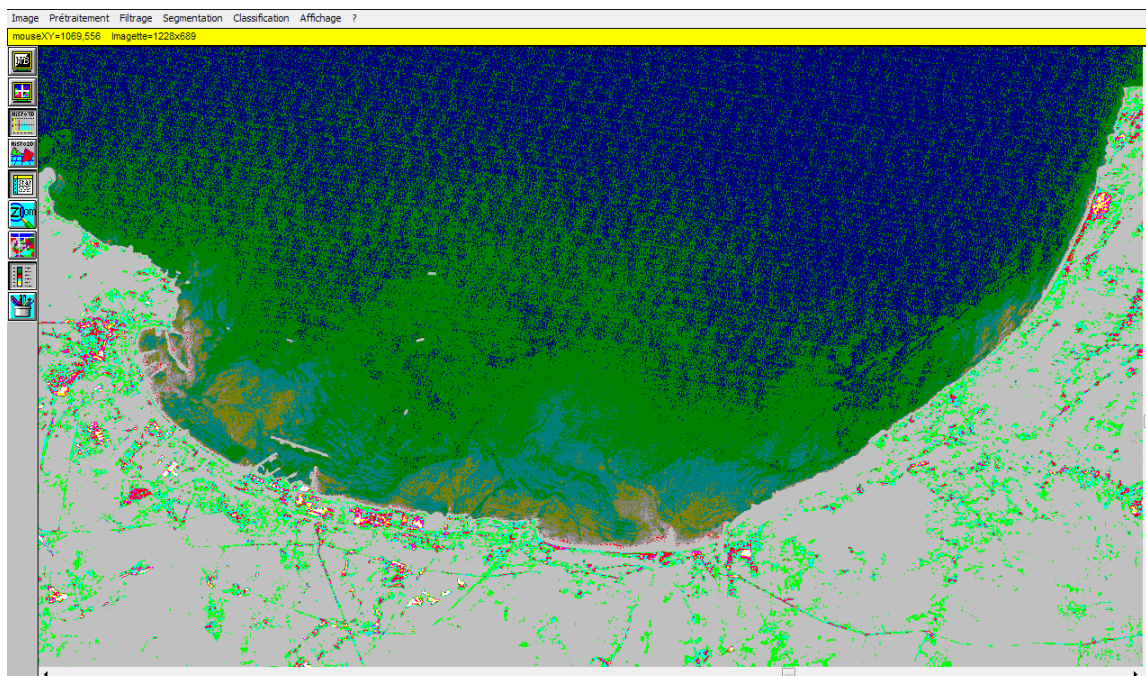


Figure 16. Variation of chlorophyll a on a SPOTXS satellite image of the Algiers Bay. (10 April 2009) $\text{Ref}(X_{S1}) = 0,17 \cdot \ln(\text{Chlr}) + 0,692$ $r^2 = +0,89532$

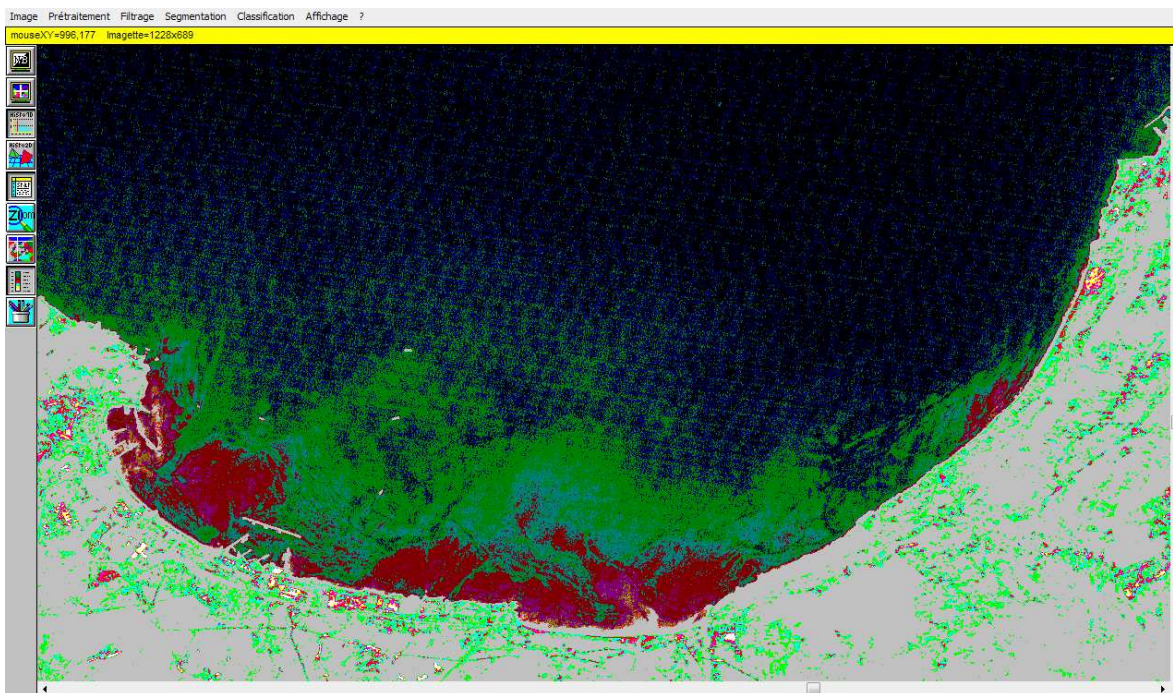


Figure 17. Variation of diatoms on a satellite image SPOTXS of Algiers Bay $Ref (SPOT_{XS1}) = 26,311 + 51,135 * C \text{ diatom} ; r^2 = 0,8920$.

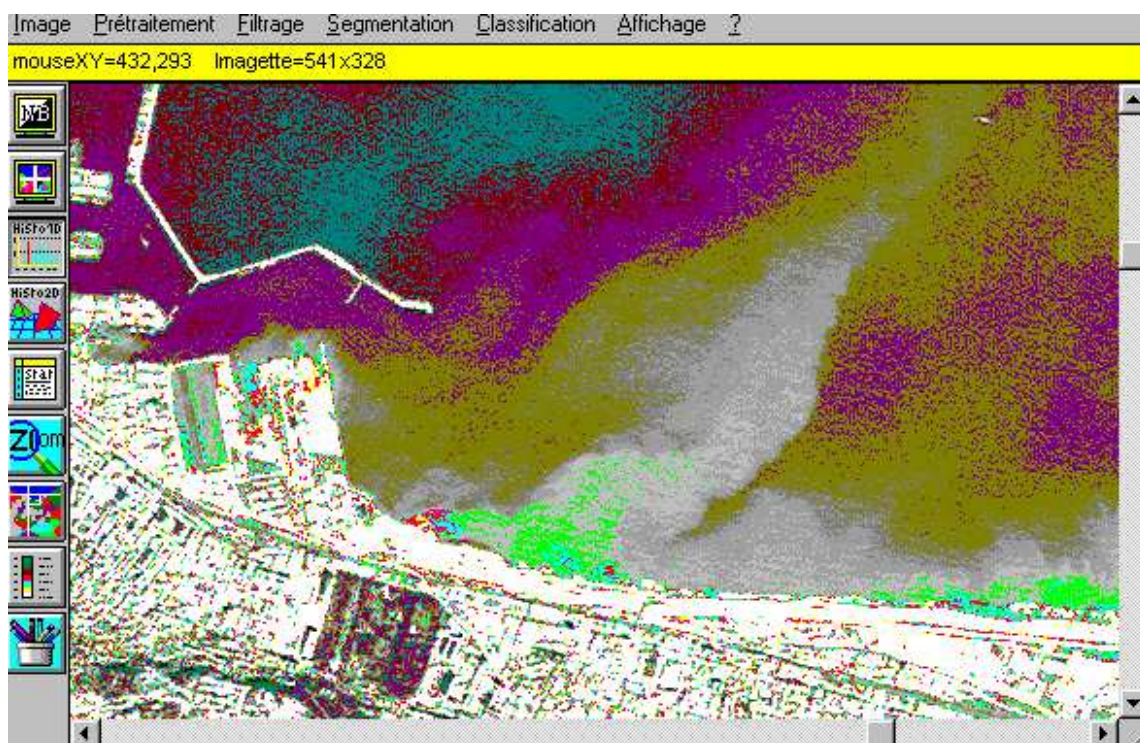


Figure 18. Variation of turbidity on a SPOTXS satellite image of Algiers Bay. (Mars, 2009) $Turbidity(NTU) = 315,9 Ref (XS1) - 1,670 ; r^2 = +0,88567$

A statistical analysis is applied between reflectance measured from satellite image and HPA (polyaromatic hydrocarbons) /HT (total hydrocarbons). It is found that the linear adjustment gives the best results on the first channels of the satellites. Comparing between the correlation coefficients, we identify adequate field of the electromagnetic spectrum necessary to study or identify a parameter related to the sea water pollution. A strong connection is thus obtained in our case among reflectances in the domain of the visible. However, it seems that the correlation is better for XS1 than XS2, and XS2 than XS3 on the satellite SPOT HRV. Landsat TM gives a strong connection on the first two channels while sensor MSS4 presents only the channel interesting for our application. Spectral bands XS1, TM1, TM2 and MSS1 give the best coefficients of correlation with corresponding reflectances Ref (XS1), Ref (TM1), Ref (TM2) and Ref (MSS1). They are thus best adapted for the follow-up of the quality of water. The lowest values are observed on channels XS3, TM5, TM6, MSS6 and MSS7 what is entirely logical since the absorption of water becomes very significant in this infra-red band, on the other hand the diffusion of the radiation becomes very weak and almost negligible what decreases the information acquired by the sensors.

Functions	Adjustment Lines Linear regression	Correlation coefficient
Ref. (XS1) = F (HPA)	Ref. 1 = 0.031505 + 0.031 * HPA	R = 0.75123
Ref. (TM1) = F (HPA)	Ref. 1 = 0.08239 + 0.0352 HPA	R = 0.85845
Ref. (TM2) = F (HPA)	Ref2 = 0.07104 + 0.0284 HPA	R = 0.7554
Ref. (XS1) = f(HT)	Ref1 = 0.041424 + 0.06 * HT	R = 0.79704
Ref. (TM1) = f(HT)	Ref1 = 0.06313 + 0.0147 * HT	R = 0.87514
Ref. (TM2) = F (HT)	Re2f = 0.04358 + 0.0118 * HT	R = 0.79823
Ref. (MSS1) = F (HT)	Ref. 4 = 0.06948 + 0.00130 * HT	R = 0.7696

Table 5. Correlation- reflectance hydrocarbons

6. Correlative analysis

6.1. The punctual measurements

All the correlations are carried out considering that the parameters are normal at 95%. It is found that the linear adjustment gives the best results on the first channels of the satellites. Comparing between the correlation coefficients, we identify adequate field of the electromagnetic spectrum necessary to study or identify a parameter related to the sea water pollution. A strong connection is thus obtained in our case among reflectances in the domain of the visible.

However, it seems that the correlation is better for XS1 than XS2, and XS2 than XS3 on the satellite SPOT HRV. Landsat TM gives a strong connection on the first two channels while sensor MSS4 presents only the channel interesting for our application.

Spectral bands XS1, TM1, TM2 and MSS4 give the best coefficients of correlation with corresponding reflectances Ref (XS1), Ref (TM1), Ref (TM2) and Ref (MSS4). They are thus best adapted for the follow-up of the quality of water. The lowest values are observed on channels XS3, TM5, TM6, MSS6 and MSS7 what is entirely logical since the absorption of water becomes very significant in this infra-red band, on the other hand the diffusion of the radiation becomes very weak and almost negligible what decreases the information acquired by the sensors.

Functions	Adjustment Lines Linear regression	Correlation coefficient
Ref. (XS1) = F (HPA)	Ref. 1 = 0.31505 + 0.0031 * HPA	R = 0.80123
Ref. (TM1) = F (HPA)	Ref. 1 = 0.08239 + 0.00352 HPA	R = 0.79845
Ref. (TM2) = F (HPA)	Ref2 = 0.07104 + 0.00284 HPA	R = 0.80254
Ref. (MSS4) = F (HPA)	Ref4 = 0.07769 + 0.00313 * HPA	R = 0.80129
Ref. (XS2) = F (HPA)	Ref2 = 0.24882 + 0.0015 * HPA	R = 0.38034
Ref. (TM4) = F (HPA)	Ref4 = 0.15979 + 0.0069 * HPA	R = 0.39720
Ref. (TM5) = f(HPA)	Ref5 = 0.26010 – 0.008 * HPA	R = 0.1579
Ref. (TM3) = F (HPA)	Ref3 = 0.11821 + 0.0135 * HPA	R = 0.38502
Ref. (MSS6) = f(HPA)	Ref6 = 0.19936 + 0.0059 * HPA	R = 0.39132
Ref. (XS1) = f(HT)	Ref1 = 0.31424 + 0.00013 * HT	R = 0.79704
Ref. (TM1) = f(HT)	Ref1 = 0.7313 + 0.00147 * HT	R = 0.79514
Ref. (TM2) = F (HT)	Ref2 = 0.06358 + 0.00118 * HT	R = 0.79823
Ref. (MSS4) = F (HT)	Ref. 4 = 0.06948 + 0.00130 * HT	R = 0.79696
Ref. (XS2) = f(HT)	Ref2 = 0.24846 + 0.00006 * HT	R = 0.42552
Ref. (MSS6) = f(HT)	Ref6 = 0.19842 + 0.00018 * HT	R = 0.35870
Ref. (TM4) = F (HT)	Ref4 = 0.15887 + 0.00020 * HT	R = 0.33988
Ref. (TM5) = F (HT)	Ref5 = 0.25454 + 0.00032 * HT	R = 0.18558
Ref. (MSS5) = F (HT)	Ref5 = 0.15067 + 0.00037 * HT	R = 0.42287

HPA: polyaromatic hydrocarbons; HT: total hydrocarbons

Table 6. Correlation between reflectance and Hydrocarbon contents.

- Pollution map

By using software PCSATWIN we have transformed the reflectance image into an image which makes it possible to estimate a certain extent the pollution of the environments by hydrocarbons. Indeed, there is a strong relation between the reflectances and these components content. Actually, the colour of sea water which is one of the obvious organoleptic descriptors, remains always a significant factor of differentiation which informs about the gleam of water, about its quality and which can be useful like an indicator of its transparency.

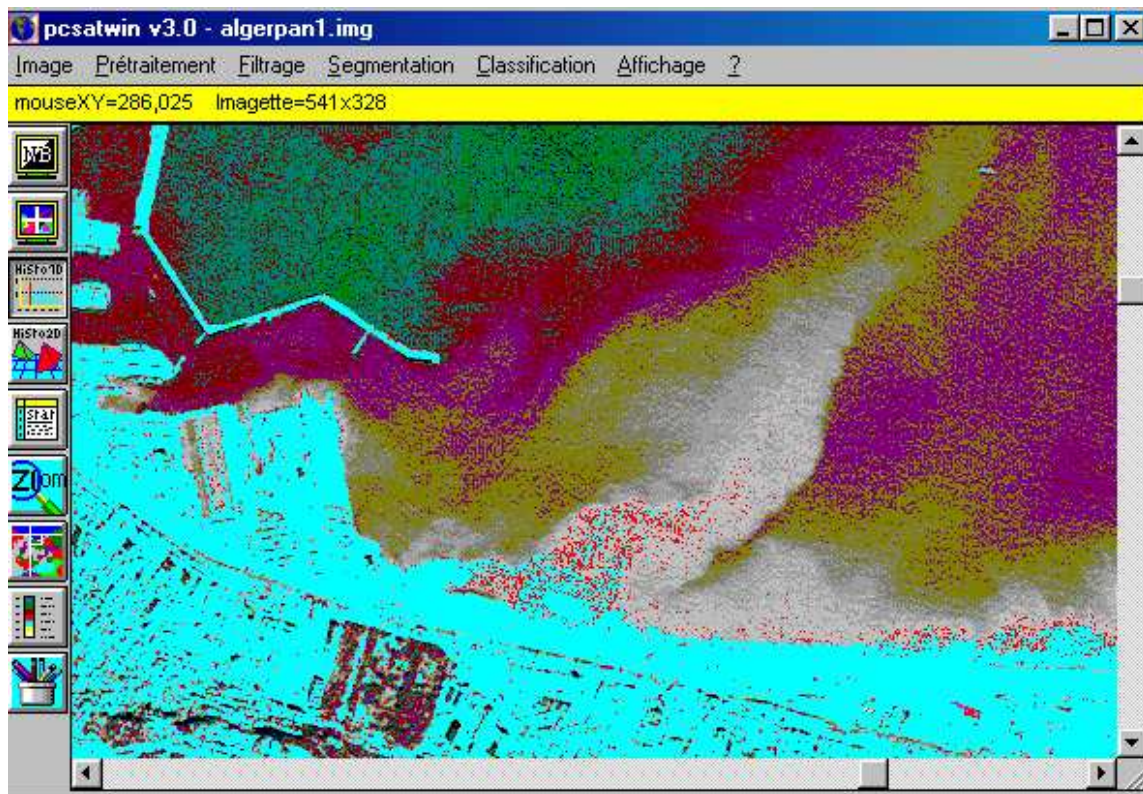


Figure 19. Spatialization of polyaromatic Hydrocarbons. Image SPOT transform starting from the relation: $HPA(\mu\text{g/l}) = -658.5 + 2092.8 * XS1$.

The figures 18, and 19, enable us to clearly classify the zones polluted by the distinction of the colour of each area on the basis of the transformed satellite image, that is to say several classes observed indicating a different degree of pollution. We conclude that the visible channels can thus be well intended for the marine applications.

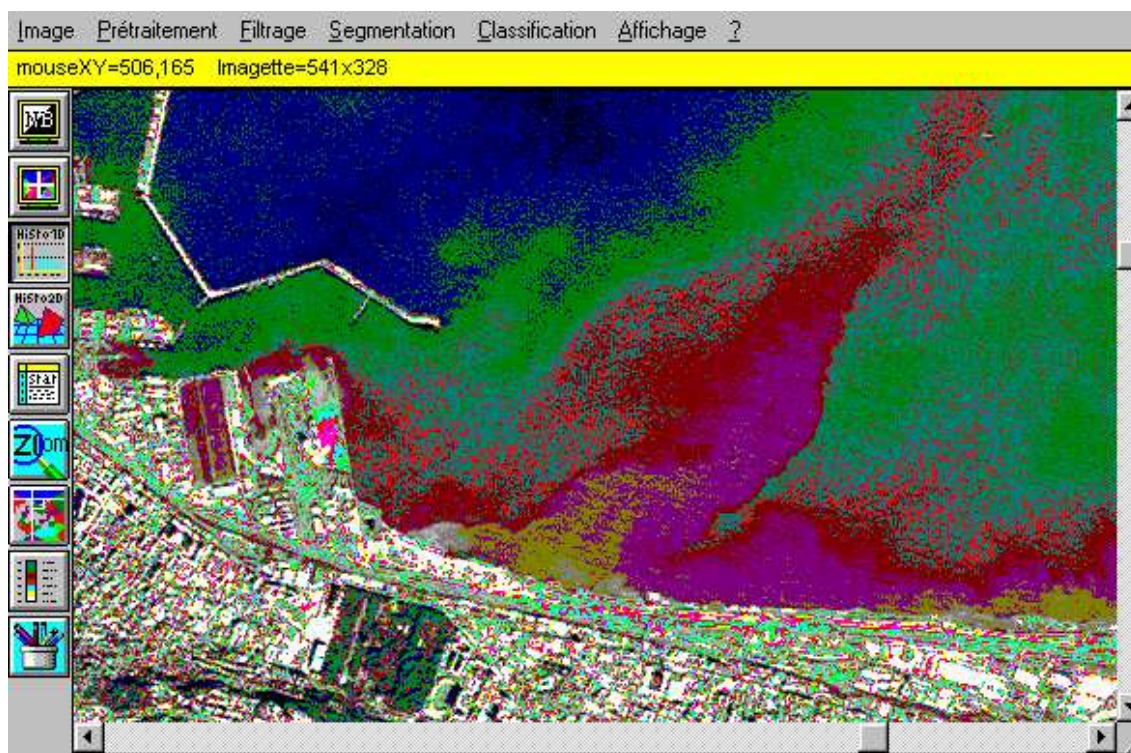


Figure 20. Spatialization of total Hydrocarbons. Image SPOT transform starting from the relation: $HT(mg/l) = -1559 + 4975.3 * XS1$.

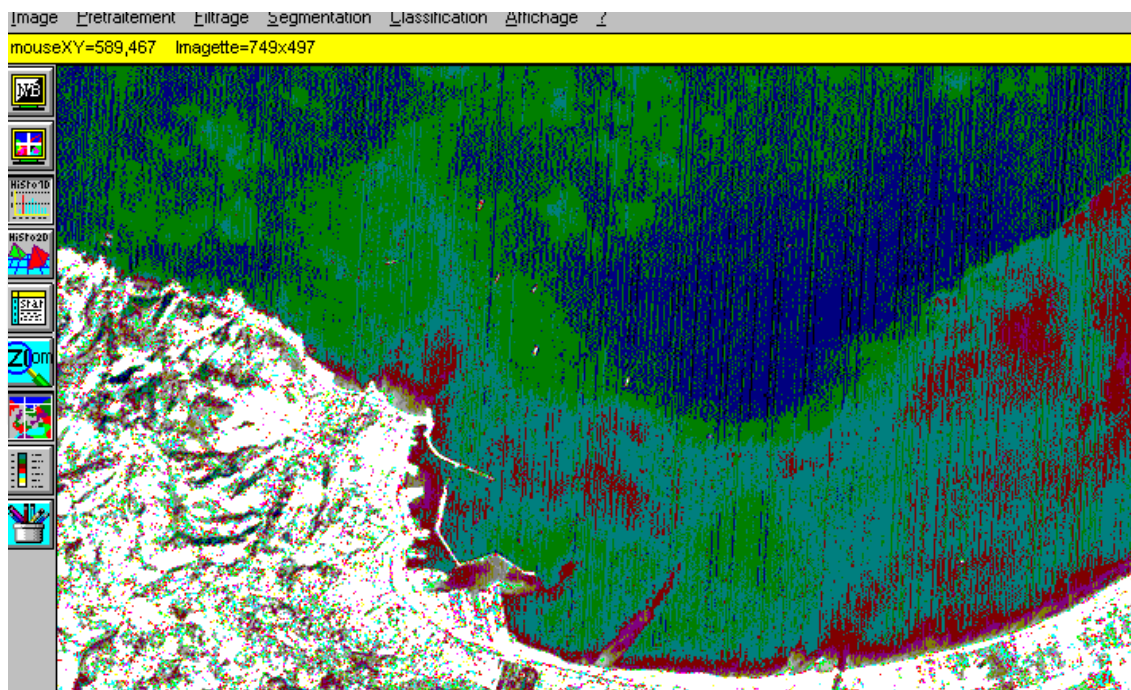


Figure 21. Spatialization of total Hydrocarbons. Image Landsat MSS transform starting from the relation: $HT(mg/l) = -29.59 + 487.83 * MSS4$.

- Pollution map

Finally, linear relations are established between physico-chemical parameters and reflectances. The inversion of these relations offers the possibility to estimate for each pixel the degree of water quality. Figures showed clearly different distinct colour subareas in each of the studied area. Each colour indicates a different degree of water quality or pollution. By this technique it is possible to construct a very beautiful and global picture for degree of unknown pollution spread over a wide water surface with relatively rapid evaluation.

By using software PCSATWIN (Bachari, 1994), we have transformed the reflectance image into an image which makes it possible to estimate a certain extent the pollution of the environments. Indeed, there is a strong relation between the reflectances and these components content. Actually, the colour of sea water which is one of the obvious organoleptic descriptors, remains always a significant factor of differentiation which informs about the gleam of water, about its quality and which can be useful like an indicator of its transparency. (Houma and al, 2004)

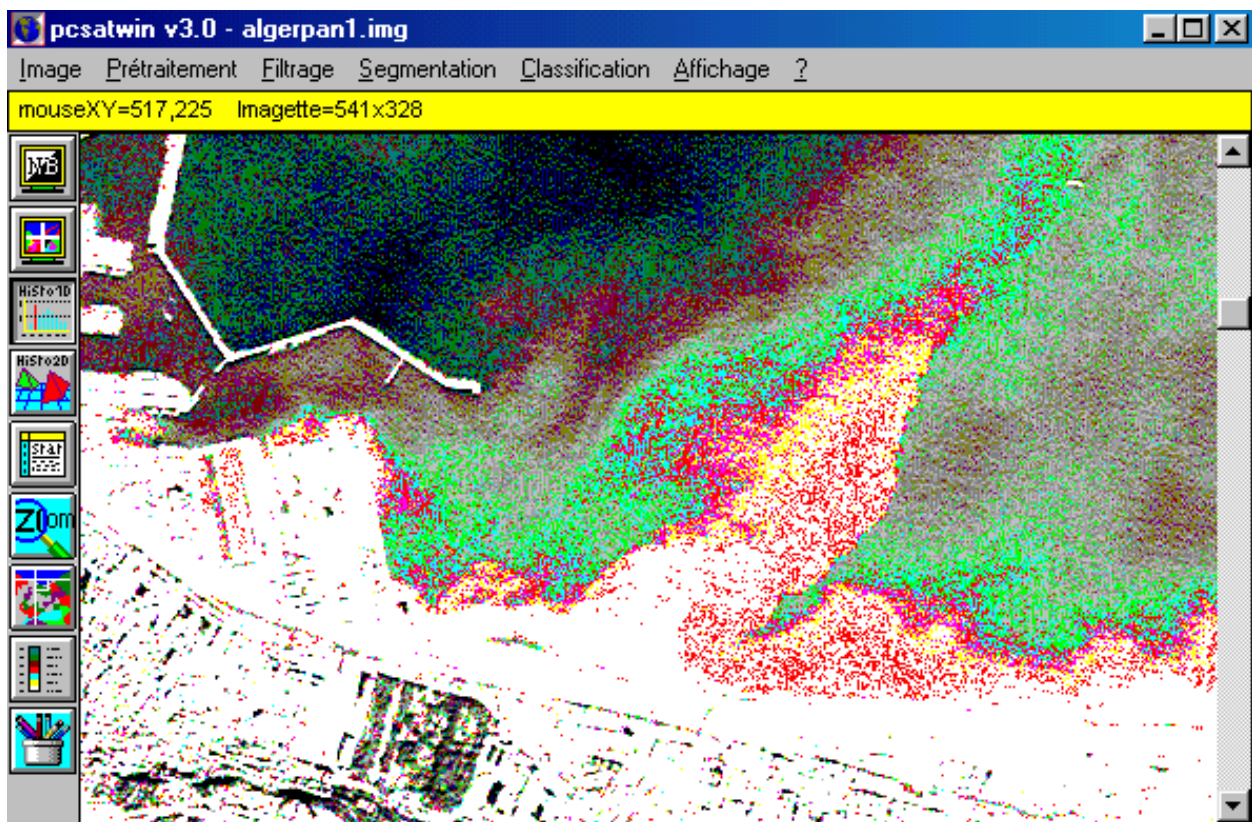


Figure 22. Spatialization of suspended matter. Image SPOT transform starting from the relation: $MES (mg/l) = -4277 + 13680 * XS1$.

The figures 20, 21 and 22, enable us to clearly classify the zones polluted by the distinction of the colour of each area on the basis of the transformed satellite image, that is to say several

classes observed indicating a different degree of pollution. We conclude that the visible channels can thus be well intended for the marine applications.

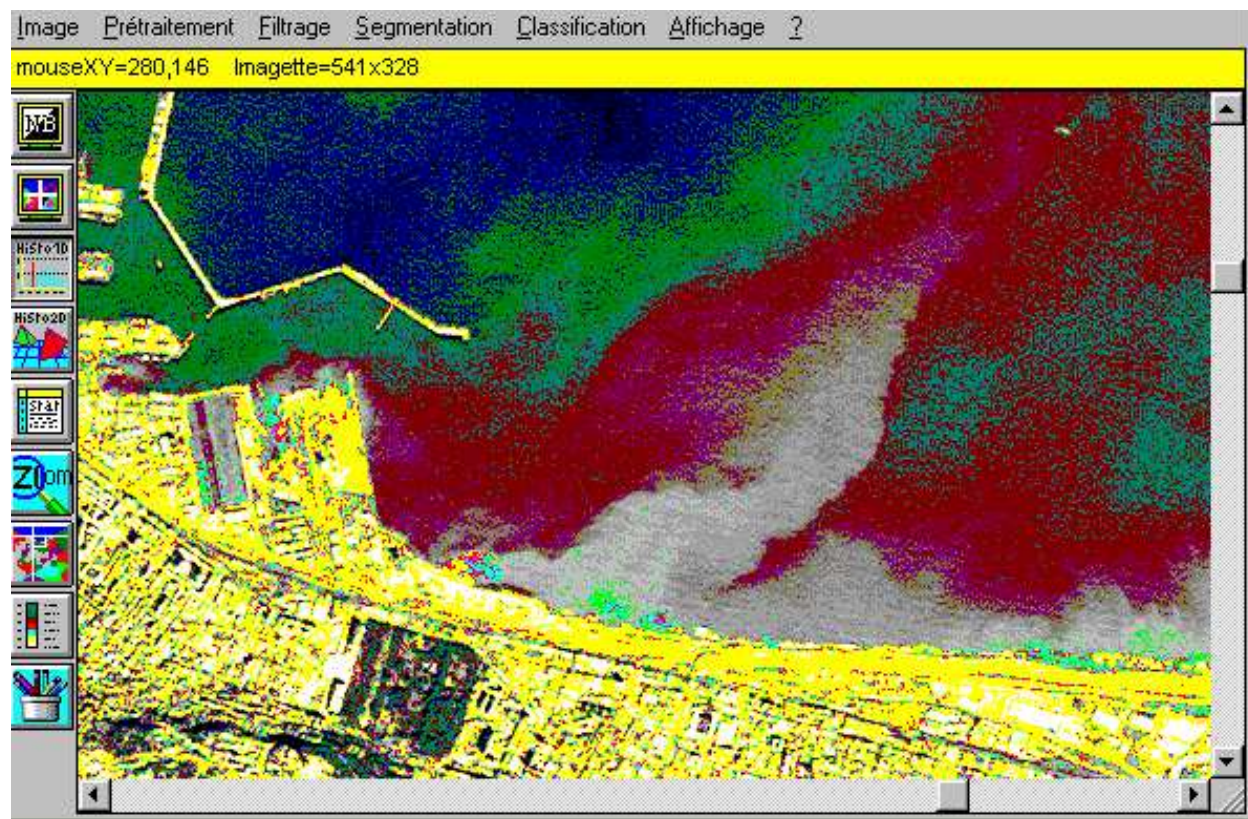


Figure 23. Variation of turbidity on SPOT satellite image XS1 of the Algiers bay $Tu (NTU) = -5149 + 16421 * XS1$.

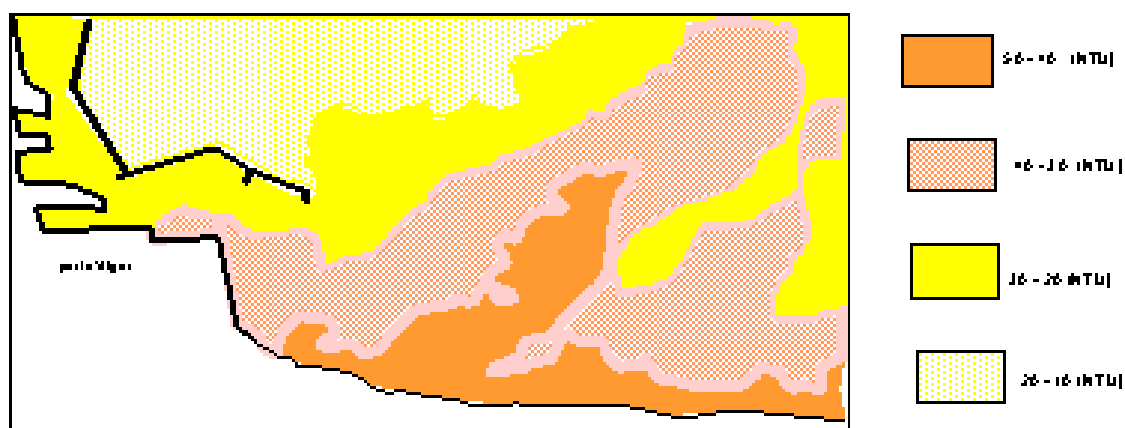


Figure 24. Cartography of the turbidity in Algiers bay.

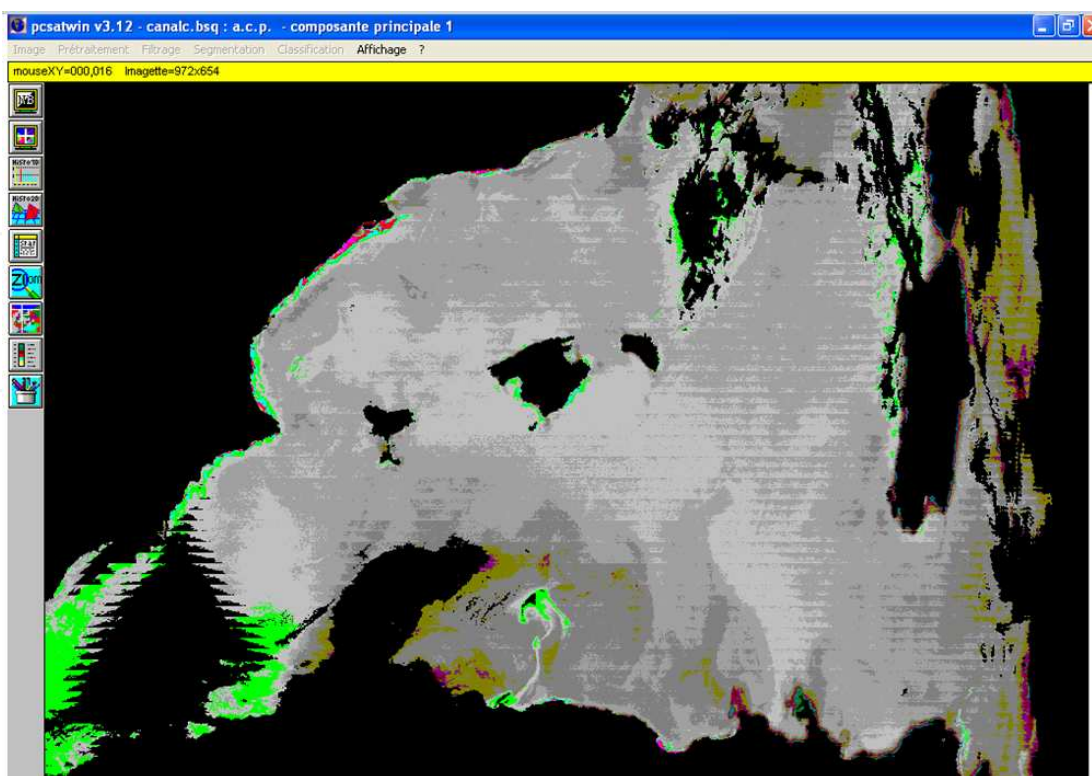


Figure 25. Chlorophyll on Channel 1 SeaWiFS

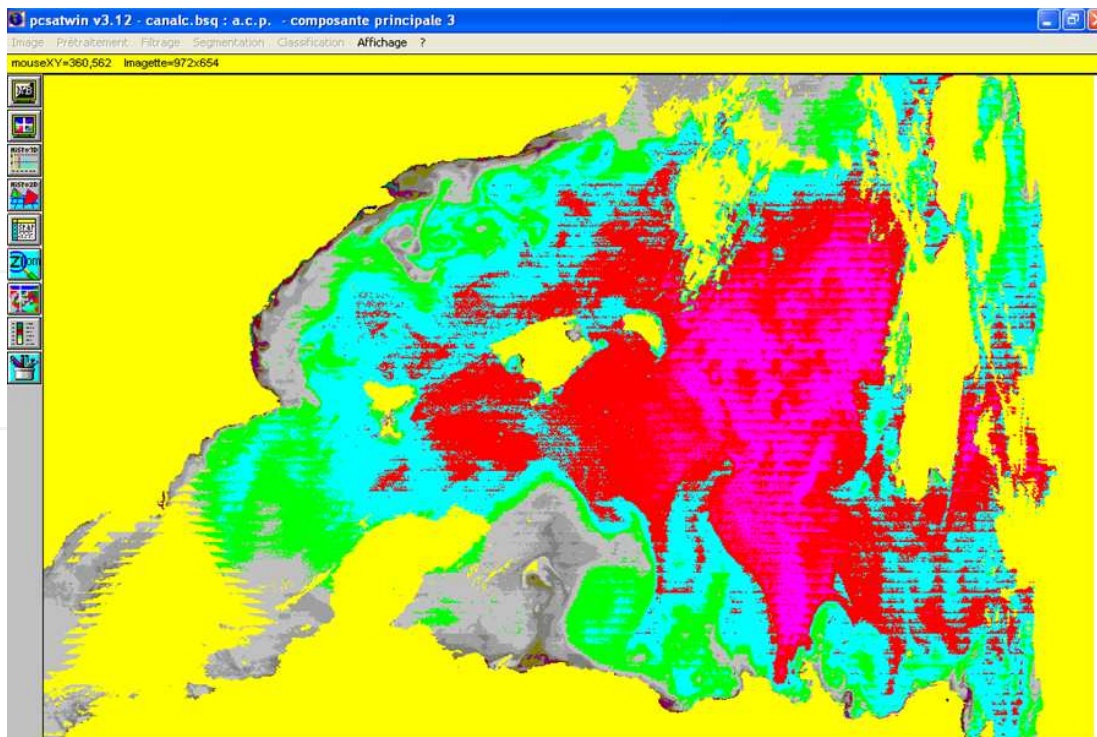


Figure 26. Chlorophyll on Channel 2 SeaWiFS

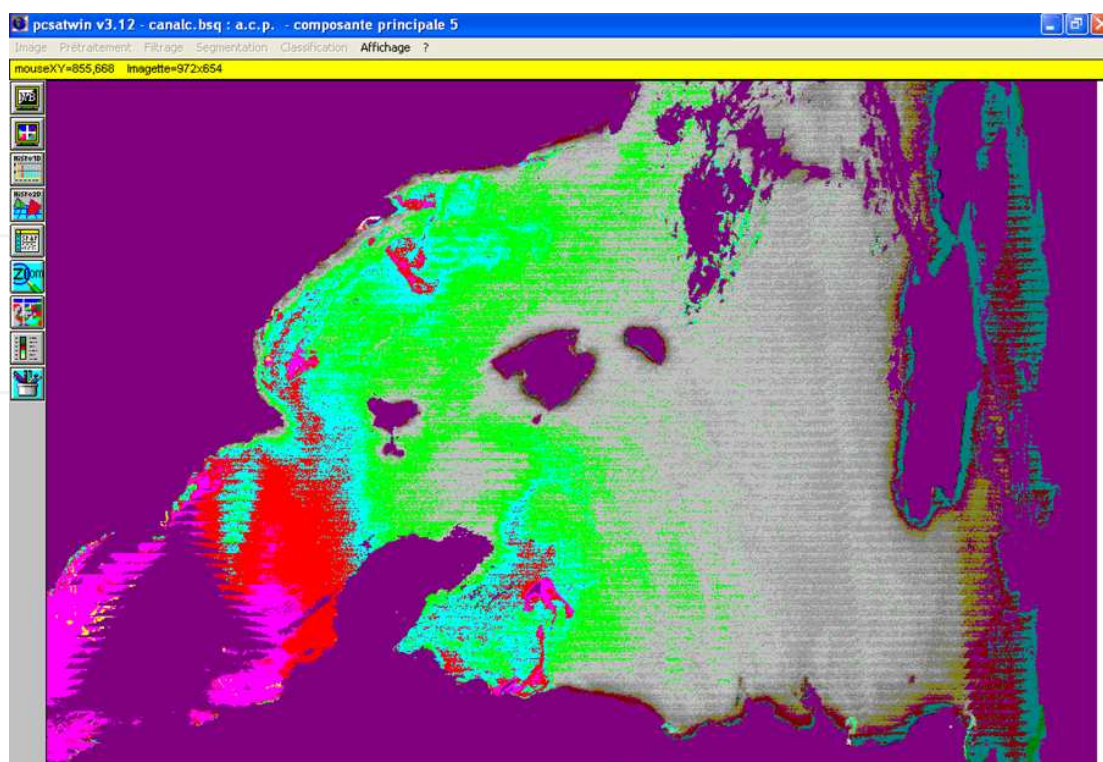


Figure 27. Chlorophyll on the Channels 4 and 5 of SeaWiFS

7. Conclusion

The SeaWiFS images (Sea-viewing Wide-Field-of-View) covering the western basin of the Mediterranean (case1 waters) comprising a part of northern Africa and southern European coasts, are treated for spatialization of the chlorophyll. The raw images of the six visible channels have been corrected for atmospheric effects.

The results of the following images correspond at consecutives scenes treated by PCSAT-WIN software. (Bachari et al., 1997)

The analysis of water sea can be a great importance for the environmental study of a given medium. The physicochemical parameters are revealing of a degree of pollution marine, but their measurements are long and very costly to be used for a continuous survey of the environment. Considering these difficulties the satellite imagery by its spectral wealth and global vision has all potentialities to be an ideal mean for qualitative analysis of the natural medium

The remote sensing is an effective technique for the space-time monitoring of the natural environment. Its use is very promising, it makes it possible to quickly cover a significant surface and at low expenses, by comparison with the traditional methods. This piece of work showed us the possibility of estimating certain pollutants on the basis of the satellite images which can be used to monitor the coastal zones pollution. Indeed, the image reveals a global and

instantaneous vision of the state of the environment and makes it possible to locate the sample in its environment. The correlative analysis made realizable the determination of the pollution indicators based on the satellites SPOT and Landsat. The spatialization of the values measured on the ground facilitates indeed the environmental monitoring of water quality and the environment interventions. The capacity of visible spectral bands is however very remarkable, they can be used for other thorough studies to establish true pollution maps which can give information on the quality of coastal water by the means of satellites put into orbit.

Author details

Houma Fouzia^{1*}, Bachouche Samir², Bachari Nour El Islam² and Belkessa Rabah¹

*Address all correspondence to: houmabachari@yahoo.fr; bachouche.samir@gmail.com; bachari10@yahoo.fr; belkessarabah@yahoo.fr

1 National School of Marine Sciences and Coastal Management (ENSSMAL). University Campus Delly Ibrahim Bois des Cars, Algiers, Algeria

2 Faculty of Biological Sciences, University of Science and Technology Houari Boumediene (USTHB), Algiers, Algeria

References

- [1] Bachari. N and. Belbachir, A.H (1996) Modélisation de l'interaction spectre solaire avec le système sol-atmosphère pour une mesure satellitaire; Congrès national de la physique et ses applications en Algérie Sétif 4-6 Décembre.
- [2] Bachari N, N-Benabadji , A-Abdellaoui ,1997a. Développement du logiciel d'analyse spectrale et temporelle des images satellite type SPOT, LANDSAT and METEOSAT, A.M.S.E, J Volume.38, N° 1,2, pp15-34
- [3] Bachari N.E.I., Belbachir A.H ., et Benbadji N.,1997 (b). Numerical Methods for Satellite Imagery Analysis, AMSE.,J Volume.38, N°1,2, pp 49-60.
- [4] Bachari. N and Benabadji. N, 1994 : Développement du logiciel d'analyse d'images satellite SPOT, LANDSAT et METEOSAT; J.Téledetection AUPELF-UREF, N° 24 .
- [5] Chandler, J.R. (1970) A biological approach to water quality management, J. Water Pollut. Control 69, 415-422.
- [6] G.M .Ferrani and S.Tassan. 1992. Evaluation of the influence of yellow substance absorption of the remote sensing of water quality in the golf Naples:a case study. Int.J.Remote Sensing ,1992 , Vol ,13,N 12 ,2177-2189

- [7] Graham, T.R (1965) Ann. Rept Lothians River Purif. Borard. Quoted according to Cahandler, 1970.
- [8] Fouzia HOUMA, Nour El Islam BACHARI, 2012 Solar Radiation Modeling and Simulation of Multispectral Satellite Data. *Atmospheric Models Applications*, 296 pages, Publisher: InTech Book Edited by Ismail Yucel, ISBN 978-953-51-0488-9, Hard cover, 296 pages, Publisher: InTech, Published: April 04, 2012 under CC BY 3.0 license, in subject Oceanography and Atmospheric Sciences, DOI: 10.5772/2012
- [9] Houma F., Bachari N.E.I., Belkessa R., and Abdellaoui A, 2010. Contribution of Multispectral Satellite Imagery to the Bathymetric Analysis of Coastal sea bottom. Application to Algiers bay, Algeria. *Journal Physical Chemical News*, volume 53(57-61), PCN, 2010.
- [10] Houma Fouzia , Khouider Ali , Bachari Nour El Islam , Derriche Zoubir ,2004 Etude Corrélatrice des Paramètres Physico-Chimiques et des Données Satellites IRS1C pour Caractériser la Pollution aquatique. Application à la baie d'Oran Algérie. *Journal Sciences de l'eau* Vol 17 No 4 pp 429-446
- [11] Houma F, Belkessa R, Bachari NEI, 2006. Contribution of multispectral satellite imagery to the bathymetric analysis of sea bottom Application to Algiers city, Algeria. *Revue des Energies Renouvelables* Vol. 9 N°3 (2006) 165 – 172.
- [12] Jaquet J.M, 1989 Limnologie et télédétection : Situation actuelle et développements futurs. *Review Sciences of water*, 2: 457- 481.
- [13] Rodier.J, (1992) L'analyse de l'eau (eaux naturelles , eaux résiduaires et eaux de mer) 7ème édition DUNOD.
- [14] Rothschein, J. (1977) Saprobität und Wasserchemismus. *Ergebn. Limnol.* 9, 101-102
- [15] Sladeczek, V. (1973) System of water quality from biological Point of view. *Ergebn. Limnol.* 7, 1-218.
- [16] Sladeczek, V. & Tucek, F. (1975) Relation of the saprobic Index to BOD5. *Water Res.* 9,791-794.
- [17] Zelinka, M. & Marvan, P. (1957) Die wichtigsten Erkenntnisse aus der statistischen Verarbeitung der Wasseranalysenresultate der mährischen flüsse. *Voda* 36, 152-155.